January 2015

Optimizing The Melanoma Tropism Of Mouse Parvovirus 1a For Use As A Viral Immunotherapy Vector

Matthew Marr

Optimizing the Melanoma Tropism of Mouse Parvovirus 1a for Use as a Viral Immunotherapy Vector

A Thesis Submitted to the
Yale University School of Medicine
in Partial Fulfillment of the Requirements for the
Degree of Doctor of Medicine

by

Matthew Joseph Marr

2015

OPTIMIZING THE MELANOMA TROPISM OF MOUSE PARVOVIRUS 1A FOR USE AS A VIRAL IMMUNOTHERAPY VECTOR. Matthew J. Marr, Peter J. Tattersall. Department of Laboratory Medicine, Yale University, School of Medicine, New Haven, CT.

Abstract:

Melanoma is a prevalent, deadly disease with poor outcomes following metastasis. It is an immunogenic cancer with many unique tumor antigens, but the tumor microenvironment inhibits the immune system. Current monoclonal antibody treatment has been shown to be beneficial in metastatic melanoma by blocking inhibitory immune signals such as PD-1 or CTLA-4. The expression of immunostimulatory proteins such as B7.1 by tumor cells could provide additional immune targeting. Viral vectors based on the parvovirus genome could efficiently and selectively express B7.1 in melanoma cells, such that they become competent to directly activate cognate T cells. Once activated, T cells will become armed as cytotoxic effectors against cells expressing melanoma tumor antigens. To generate a viral vector, we first needed a parvovirus that infected melanoma. Parvoviruses are uniquely adapted to infect tumor cells as viral replication is dependent on the host cell advancing through S phase. However, most parvoviruses tested were unable to establish infection in the murine melanoma cell line B16F10. The most infectious parvovirus in B16F10 was mouse parvovirus 1a (MPV1a). B16F10 cells were infected with MPV1a, and the progeny virus was harvested and used to re-infect more B16F10 cells. After five serial passages of virus, the mutant polyclonal stock named MPV P5 was analyzed. At 24 hours following infection at a multiplicity of 5000 virions per cell, MPV1a infected 16% of cells, whereas MPV P5 infected 74%. Construction of a molecular clone from the polyclonal MPV P5 mixture yielded a construct consisting of the non-structural and virion polypeptide (NS and VP) genes that was able to infect 45%

of cells under the same conditions. The mutations that were most responsible for the increase in B16F10 infectivity were isolated to the VP2 region, which encodes the major capsid protein. By incorporating the viral proteins from the clonal version of MPV P5 into a parvoviral vector system, we have generated a vector capable of transducing B16F10 cells and simultaneously expressing the Green Fluorescent Protein marker and B7.1. Further experiments are needed to determine if the B7.1 expression is sufficient at its current rate of infectivity to modulate an immune response, and to examine whether viral products within the tumor cells generate additional immunogenic signaling. Other aspects of the MPV P5 genome may be engineered into the vector to increase its efficiency.

Acknowledgements:

This thesis would have been impossible to complete without the wisdom and support of the Tattersall Lab. Peter has been an amazing mentor, providing an endless supply of his most valuable resource – time. His editorial skills are unparalleled, and I never found any British spellings in any of his corrections (even his late night ones), despite some serious scrutiny on my part. Sue has been an unending source of knowledge with enough papers and references to keep me going for days. Ivo has been, and will forever be, the master of the western blot and is full of many insightful observations about the English language. Lei is the efficiency queen with an omnificent understanding of protocols and the experience to make every wash step 25% faster. Chinese New Year will always be in my calendar with the hopes that I'll be passing through New Haven and can get some of the most delicious dumplings I have ever tasted. Last, is Tony. Where to start. He's quite the lab historian and cloning guru, who kept me going with his fatherly-yet-friend-like encouragement when results were less than perfect. His supply of reagents was everything you could ask for in a bench partner and he never made fun of me when my "last cloning step" was clearly not the "last cloning step." Katie Meeth, from the Bosenberg Lab, also deserves some thanks for her unbridled supply of YUMM cells, twice. As a whole, this lab has been the one constant part of medical school for me. Starting with Peter on my medical school interview day to a hopefully joyous residency match party in March, these people have seen my roller-coaster experience of the medical education system and they certainly made it more enjoyable and more fulfilling.

I would also be foolish not to thank Anna. She has endured way too much talk of viruses and waiting an additional 50% of however long I said it would take for me to split cells/pick colonies/run a quick gel. She also had to deal with me at lunch after getting plenty of negative results. Let that be a lesson to never check a PCR for the right-sized product before going to lunch with people. Time with her is way too valuable to be upset over the small stuff. I can't wait to start the next chapter of my life with her.

Lastly, the Office of Student Research provided the flexibility and funding for all of my endeavors, financing me for a cumulative year over the past two years with their short-term funding. I cannot think of a better way to experience the "Yale System" than through the amazing opportunities to go abroad, work in lab, take some electives, and comfortably apply to residency. Yale, it truly has been a wonderful nine years.

Table of Contents:

Introduction:

Approaches to Melanoma Therapy

Melanoma is a deadly form of cancer that metastasizes easily without detection and becomes incredibly difficult to treat. In 2015, the American Cancer Society expects 73,870 new cases of melanoma with 9,940 projected deaths (1). Before the advancement of monoclonal antibody treatments for metastatic melanoma, treatment was limited to decarbazine and interleukin-2. Recently, inhibitors against BRAF and mitogen-activated protein kinase kinase (MEK) have been shown in the clinic to suppress tumor growth. New monoclonal antibodies are targeted at deconstructing the immune evasion signals that melanoma evokes for survival. In the realm of immunotherapy, as summarized in Figure 1 (2), the CTLA-4 inhibitor ipilimumab is currently approved for melanoma treatment, along with interleukin-2 and interferon. Signaling mechanisms currently being targeted in this way include inhibiting programmed cell death receptor (PD-1), activating CD27 (TNF stimulatory receptor on T cells), inhibiting B7-H3 (possible B7 inhibitory signal), inhibiting phosphatidylserine exposed on the outer surface of the cell membrane, and increasing granulocyte macrophage colony stimulating factor. Another aspect of immunotherapy is being addressed by the development of cancer vaccines, using antigenic proteins from melanoma, such as melanoma antigen-1 (MAGE1), GP100, Melan A, NY-ESO, or autologous tumor lysates to stimulate the immune system. The remaining immunotherapy under investigation is adoptive T cell therapy, where lymphocytes found invading the tumor are removed, expanded, and returned in much greater numbers (2).

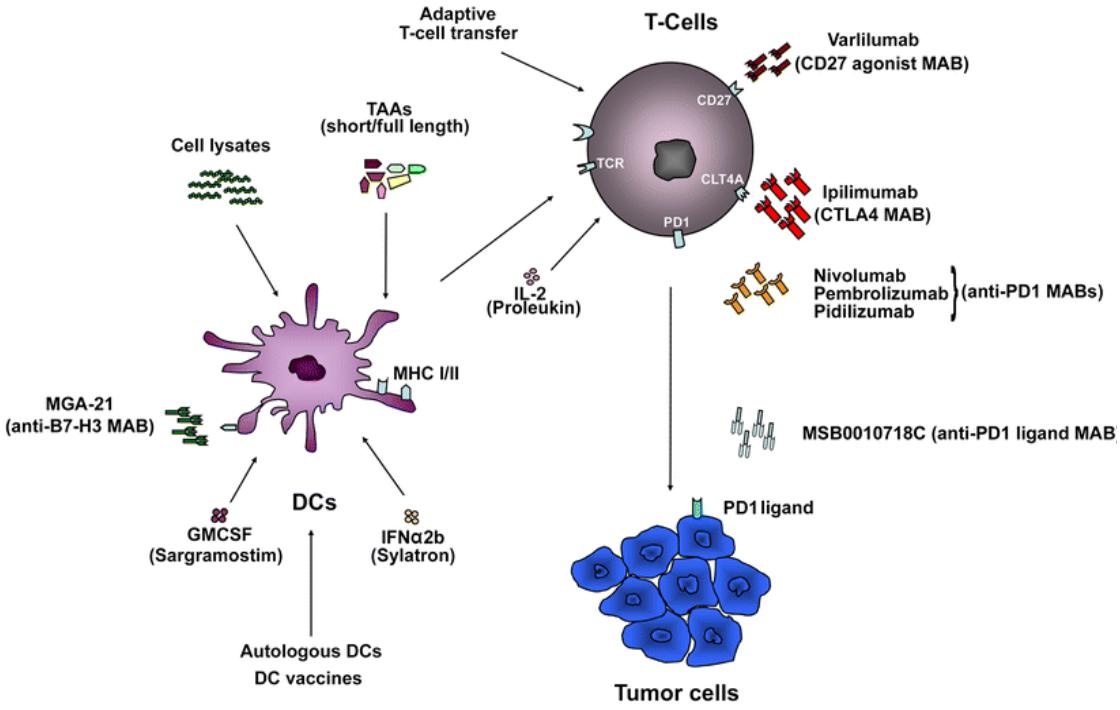

Figure 1 – Summary of Cancer Immunotherapies

Multiple interactions exist between tumor cells, T-cells, and dendritic cells (DCs) that modulate the immune response to cancer cells. Current receptors and medications are summarized above in a figure from Rotte et al (2).

This project aims to complement some of these immunotherapeutic approaches by developing a parvoviral vector that expresses B7.1/CD80 in melanoma cells to generate its proposed immunostimulatory effect (Figure 1). B7.1 is part of the B7 family of ligands that are involved in stimulatory and inhibitory immune signaling. In the canonical sense, antigen presenting cells (APCs) present an antigen on MHC to the T cell receptor (TCR) of a naïve T cell. This interaction is reinforced by B7.1 on the APC binding to the CD28 receptor on the naïve T cell leading to increased proliferation and induction of the cytotoxic T cell phenotype in an activation process known as co-stimulation. As the T cell matures, it switches to express the inhibitory receptor CTLA-4 (cytotoxic T-lymphocyte-associated protein 4), which binds to B7.1 with a higher affinity

than CD28, and thus limits CD28's proliferative signaling. Other ligands found on tumor cells can also modulate the growth and activity of T cells. Programmed death ligand 1 (PDL-1) is another immune signal commonly found on tumor cells and binds the PD-1 receptor on activated T cells in peripheral tissues. This event is a late inhibition of activated T cells as compared to the early inhibition of function by CTLA-4. Expression of PDL-1 is a negative prognostic factor for survival (3).

The idea of using B7.1 expression in cancer cell lines has been promising in previous studies. The administration of non-replicating immunogenic tumor cells expressing B7.1 increased survival against future tumor challenges when B7.1 was expressed (4). The human melanoma cell line Me1B6 leads to increased lymphocytic cytotoxic activity and cytokine release when expressing B7.1 (5). UV-induced melanoma K1735 expressing B7.1 leads to a 90-day immunity against re-challenge in mice (6). The response to B7.1-expressing tumor cells can be augmented by co-treating with IL-12 to improve activity against poorly immunogenic tumor types (7). B7.1 expression has been shown to overcome the protective effect of tumor cells expressing PDL-1 on the surface (8). Given the previous success of B7.1 in melanoma, we would like to use a parvoviral delivery system to express B7.1 in tumor cells, so that the B7.1 can activate T cells to become cytotoxic effectors and the viral proteins can increase the immunogenicity of the signaling.

The Genetic Strategy of Parvoviruses

Parvoviruses are single-stranded, non-enveloped DNA viruses. The genome is quite small, approximately five kilobases in length. Two tandemly arranged gene cassettes encode for the nonstructural (NS) proteins and viral capsid proteins (VP). Splicing of the major intron allows for two major non-structural proteins variants, known as NS1 and NS2, as shown in Figure 2 (9). Alternative splicing within the central, minor intron region generates two VP gene products, VP1 and VP2, which differ at their N-termini by the inclusion of a 142 amino acid peptide called the VP1 specific region (VP1SR). The minor intron alternative splicing also generates three isoforms of NS2 that differ in their C-terminal hexapeptides. At the end of the VP2 gene there is a 3' untranslated region (UTR) that, in some viruses, contains internal repeats. Infection occurs when the virus enters the cell and the viral genome is converted into double-stranded DNA in the nucleus, allowing transcription from the initiating P4 promoter, leading to production of NS1 and NS2 as early nonstructural proteins. Accumulation of NS1 will then lead to production of VP1 and VP2 capsid proteins from the P38 promoter. The genome is amplified through a process of rolling hairpin replication, in which hairpins on the ends of the single-stranded genome self-prime the genome for extension by host cell polymerases. This process continues unidirectionally to produce double-stranded multimeric intermediates that are cleaved into monomer lengths from which single-stranded genomic units are "peeled off" for packaging. Once the viral genome is packaged into the assembled capsid, it is exported out of the nucleus and cell (10).

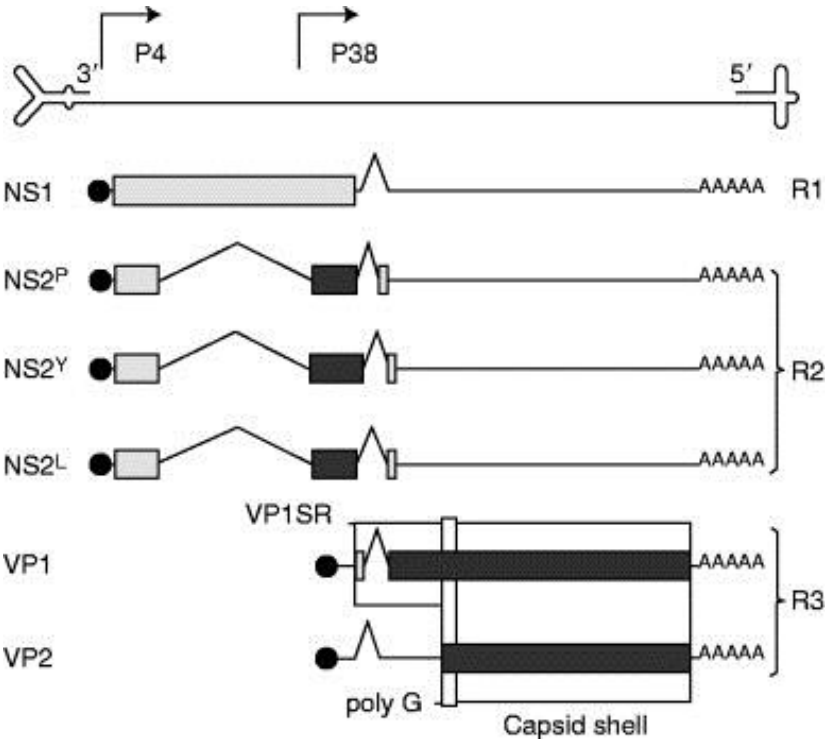

Figure 2 – Rodent Parvovirus Gene Products, Reading Frames, and Splicing

This figure demonstrates the genetic organization of parvoviruses adapted from Cotmore et al (9). Non-structural protein 1 (NS1) is located within the first reading frame. Three splicing variants of NS2 are in the second reading frame. Two splicing variants of the VP gene are in the third reading frame and produce the capsid. The P4 promoter drives the production of NS1/NS2, while NS1 drives the P38 promoter to make the VP peptides.

Parvoviruses lack an intrinsic process for initiating the conversion of their packed single-stranded DNA into double-stranded DNA, and until the cell progresses through S phase, the genome appears to remain sequestered in the capsid and incapable of transcription. Unlike other DNA viruses, the parvoviruses do not possess any early-acting ancillary proteins that can coax the non-cycling host cell into S phase, so they must wait until the cell prepares to divide (11), thus they are innately primed to replicate in rapidly-dividing cells, making them uniquely suited for targeting malignancy.

However, the mechanism(s) underlying the inherent oncotropism of parvoviruses are more complex than the S phase requirement, which can be met by any dividing cell. Current research indicates that normal human cells are able to suppress rodent parvoviral infection while transformed cells lose that ability. In infections with the most intensely studied prototype parvovirus Minute Virus of Mice (MVMp), transformed A9 mouse fibroblasts fail to express type 1 interferon and become infected, while non-transformed murine embryonic fibroblast precursors do release interferon to combat infection (12). However, this observation cannot be extrapolated to human cells, since other studies have shown that interferon does not affect parvoviral infection in either normal or transformed human cells (13, 14).

The idea of using viruses to treat cancer is not new. Originally, the goal was to use oncolytic viruses to directly lyse the malignant cells. Cervical cancer regression was seen with rabies infections in 1912 and clinical trials treated cervical cancer with adenovirus with moderate success in 1954 (15). The most current oncolytic treatment of melanoma with viruses uses herpesvirus or coxsackie virus engineered for cancer cell specificity and GM-CSF expression in the tumor (16). Treatment ideas have shifted as technology advanced and gene delivery via viral vectors became possible. Propagating, infectious particles can be replaced with highly-engineered vector systems. These vector systems remove the fear of propagation and allow the expression of transgenes, as elaborated in the following section.

Development of Parvoviral Vectors

Autonomously replicating parvoviral vectors (Figure 3) can be produced with transgenes up to ~2.5kb in length and can be supplied with modified capsids to influence tissue specificity (17). They can provide transient gene transduction in dividing cells with low risks for unintended consequences due to their inherent oncotropism and lack of viral incorporation into cellular DNA (18). The lack of human immunity to rodent parvoviruses means that the vectors will not be immediately inactivated by preexisting neutralizing antibodies (19).

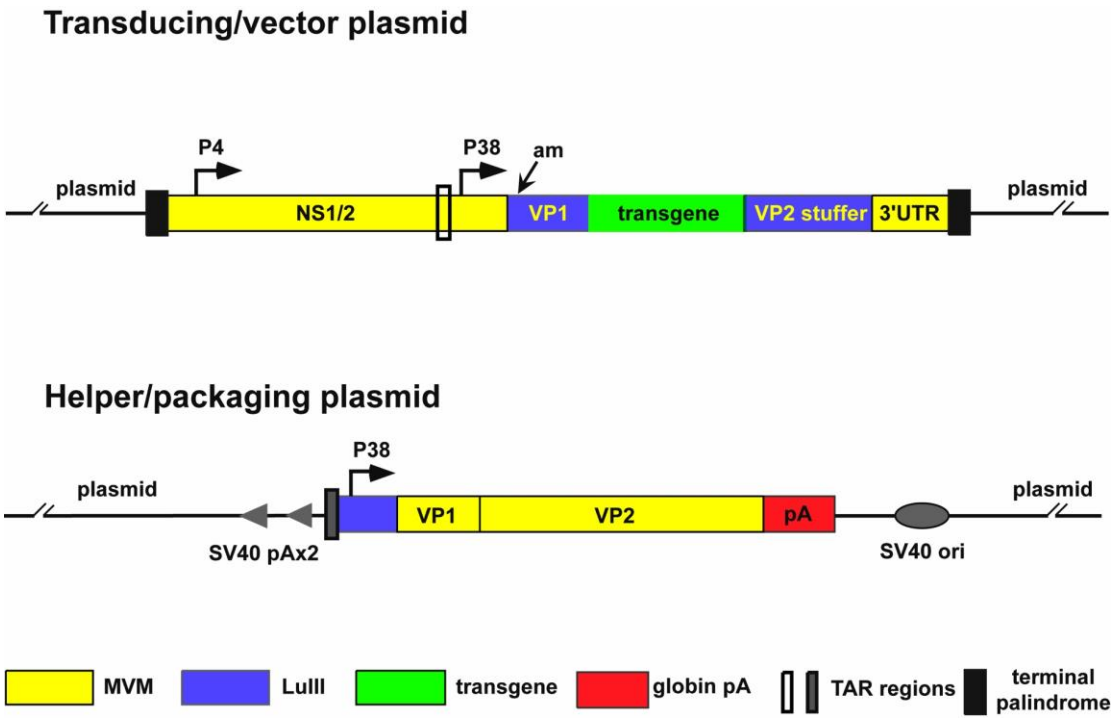

Figure 3 – The Original Autonomous Parvoviral Vector System

The vector plasmid has an early stop codon at the start of truncated VP1 so no capsid proteins are expressed. The transgene fits into the remaining space from the VP1 truncation. VP2 stuffer sequence is added as needed to bring the overall construct length into the appropriate 5 kb size for DNA packaging into the capsid. The packaging plasmid expresses VP1/VP2 in trans from the P38 promoter to provide a capsid for the vector genome to be packaged.

Generating an effective vector system requires starting with a competent virus from which to build. Mutagenesis and selection have been performed on many parvoviruses to study the changes in tropism and map mutations that lead to new cell type infectivity. Changes in tropism arise from many aspects of the viral genome. For example, the parvovirus MVMi, which happens to be lymphotropic, can infect fibroblasts when two amino acids changes are made in the capsid gene that mimic the capsid of MVMp, as selected by plaque assays of MVMi on A9 mouse fibroblasts (20). Other studies have shown that while MVMp and MVMi will not undergo lytic growth in the other cell's permissive cell line, both viruses can enter and convert into double-stranded genomes in both cell lines, indicating that some cellular factors are limiting the virus's ability to infect despite entering the cell with two different capsids (21). The P4 promoter leading to the transcription of NS1 has also been shown to influence tropism (22). These three leading options of capsid, non-structural protein, and P4 promoter mutations have become the focus of a search for a more melanoma-tropic parvovirus.

The parvovirus LuIII has been shown to infect primary human melanoma cell lines, but unfortunately does not infect murine melanoma cell lines (23). The finding that LuIII selectively infects human melanoma cells is what sparked this project in the first place, since we would need a mouse model to further develop a parvovirus-derived LuIII vector for humans. While most members of the rodent parvovirus panel we have assembled are unable to grow in the well-characterized B16F10 mouse melanoma cell line, Mouse parvovirus 1a (MPV1a) was found to be the best candidate for infecting these cells. As shown by a simple screening test, infection by this virus was rather inefficient, however the other parvoviruses showed no infection. MPV1a is in the same

species as LuIII and MVMp, known as rodent protoparvovirus 1 within the genus *Protoparvovirus* (24). This is significant because many of the genomic templates, techniques and assays, as well as much of our understanding of parvovirus biology, stem from studies on MVMp, and hopefully another parvovirus derived from MPV1a in the same species would behave similarly. Also, the similarity between MPV1a and LuIII might imply that the discoveries made with MPV1a in a murine melanoma model could be translated to human melanoma via LuIII. By starting with MPV1a, we set out to create a parvovirus that would infect B16F10 cells just as LuIII infects human melanoma cells. Parvoviral replication yields a single nucleotide mutation for every 10^4 bases (12). So, with a 5000 bp genome, on average every other viral genome should have a mutation within it. While many will be silent or deleterious, selection on B16F10 cells should occur rapidly, yielding quasi-species of mutant MPV1a parvovirus with new levels of melanoma infectivity. We passaged MPV1a on B16F10 cells, infecting the cells and harvesting the progeny, which were then used to re-infect and select for more competent mutants. This selection process was repeated five times, resulting in a polyclonal mixture of mutant MPV1a that was named MPV P5 (passaged five – P5). MPV P5 became our window into understanding how to target parvoviruses to murine melanoma with the hopes of generating a vector for treatment purposes. Genetic traits found in the MPV P5 virus can be applied to vector system to make it as efficient as possible.

One of the possible advantages of using a replication-competent, but non-propagating viral vectors is that the immunostimulatory response from vector transduction is likely to be higher than simply expressing B7.1 in a non-replicating vector. Although the vector will not create new viral particles, NS1 will still be

expressed to high levels. While parvoviruses can avoid triggering some cellular defenses, such as Toll-like receptor 9 (TLR9) failing to detect the incoming viral DNA in plasmacytoid dendritic cells (25), infected cells do express some damage-associated molecular patterns and pathogen-associated molecular patterns (DAMPs and PAMPs). We predict that these DAMPs and PAMPs, in conjunction with the costimulatory signaling of B7.l, should result in a robust immune response to unique tumor antigens.

While B16F10 is a useful and well-characterized model for murine melanoma, both in culture and transplanted into immunocompetent C57BL/6 mice, its tumor-specific genotype does not reflect the most frequent mutations found as drivers of human melanoma. In this respect, we are fortunate to have established a collaboration with Dr. Marcus Bosenberg's group in Dermatology at Yale, who have provided us with a unique set of engineered murine melanoma cell lines that more faithfully represent the repertoire of driver mutations leading to human melanoma. The Yale University Mouse Melanoma (YUMM) cell lines developed by the Bosenberg laboratory provide a unique opportunity for testing B7.1 expression in a genetically defined tumor model both *in vitro* and *in vivo*. The first generation of these cell lines (denoted 1.x) is derived from a tumor on a mouse with a $Braf^{V600E}$/wt $Cdkn2A^{-/-}$ $Pten^{-/-}$ genotype. $Braf^{V600E}$ is a constituently active mutant. The second generation (denoted 2.1) utilizes a mutation that stabilizes β-catenin instead of the Cdkn2A knockout. Both cell lines are transplantable into C57BL/6 mice and metastasize to the lungs, providing a much more realistic model than what B16F10 cells can provide (26). While MPV P5 was not selected on YUMM cells, evolutionary advantages from growth on B16F10 cells may be equally beneficial in this other murine melanoma model and allow for rigorous, immunology-based study of the vector system.

Statement of Purpose:

Parvoviruses may be used as an efficient vector for expressing transgenes in murine melanoma cell lines. Specifically, the parvovirus MPV1a, after being passaged in B16F10 cells, has undergone genetic changes that improve its infectivity in melanoma cell lines. These mutations can be investigated by creating chimeric viruses with MPV1a and MPV P5 components, and the most important components for melanoma tropism can be applied to the vector system to improve its functionality. The vector system, when targeted to melanoma, can express immune-stimulatory signals such as B7.1 to generate an immune response against the tumor.

Aims:

1.) Clone and sequence parental MPV1a strain and resulting MPV P5 mutants
2.) Analyze differences between the two sequences to isolate potential enabling mutations for melanoma infectivity
3.) Create chimeric viruses by combining MPV1a and MPV P5 sequences to isolate mutations responsible for increased infectivity in melanoma cells
4.) Transfer enhancing mutations into the parvoviral vector system
5.) Construct GFP-B7.1 transgene in the vector system
6.) Investigate expression of transgene in melanoma cell lines with vector transduction
7.) Perform *in vivo* experiments with the vector system and monitor for a tumor-specific immune response

Methods:

Selection of MPV1a on B16F10 Cells

Performed by Peter Tattersall, the selection process occurred with plated B16F10 cells infected with MPV1a virus. After ~3 days, cells were harvested, spun down, and resuspended in Tris/EDTA (TE) buffer pH 8.7. The sample was rapidly frozen in dry ice and thawed on ice three times to release virus particles from the cells. After centrifugation, an aliquot of the supernatant containing the virus was applied to a fresh culture of B16F10 for re-infection. This process was repeated for a total of five times. The resulting virus was named MPV P5 for the five passages it underwent on B16F10 cells.

Viral sequencing

I performed the PCR cloning and sequencing of the viral genomes. Fragments of the viral genome were amplified with PCR. The parental MPV1a and MPV P5 viruses were denatured at 95°C for 10 minutes. Primers were designed from the start of NS1 to the end of VP1 and from the start of VP2 to the end of VP2. Additional primers were designed from the start of VP2 to the end of the 3' untranslated region. PCR was done with high fidelity Phusion polymerase. A-tailing of the PCR product was performed with Biolabs Taq DNA polymerase. The product was incorporating into either Topo pCR 2.1 or NEB pMiniT vectors and transformed into E. coli. All reactions and procedures were carried out according to the manufacturers' instructions. Plasmids were then sequenced by using proprietary primers for the respective cloning vectors at the Keck Sequencing Center.

Viral subcloning

I performed the subcloning of viral sequences. The NS1/NS2/VP1 sequence was isolated by digestion with PmeI and SacI restriction enzymes. The VP2 sequence was isolated by digestion with SacI and PacI. Chimeras were formed by ligating the appropriate fragments and the MVMp infectious clone backbone with NEB quick ligase and transforming into Agilent SURE-2 supercompetent cells. Terminal hairpin lengths were confirmed with AflIII digests.

Viral production

I performed the production of the viral chimeras. They were grown in 293T cells following transfection with polyethylene imine (PEI). $2x10^6$ 293T cells were plated in 100mm dishes the day before transfection. Each dish was treated with the transfection mixture of 4ug infectious clone DNA, 6ug pXX6-80 helper plasmid, and 25ul PEI. Cells were harvested after 72 hours, suspended in 500ul TE pH 8.7 per plate, lysed by repetitive freeze/thaw cycles, and the cellular debris was discarded after centrifugation. Virus production was confirmed using a hemagglutination assay where 1% guinea pig red blood cells are mixed with increasing dilutions of viral extract. Virus extract with high titers will agglutinate the RBCs and prevent them from settling to the bottom of the well, even at high dilutions.

Virus purification and quantification

Virus purification was achieved via ultracentrifugation in 15, 35, 45, and 55% iodixanol gradients, spun at 35,000 rpm for 18 hours. The gradients were fractionated starting at the highest density of 55% iodixanol. Samples were taken from each fraction and prepared for Southern blot analysis. They were treated with micrococcal nuclease,

Proteinase K, and 10% SDS sequentially and run in an alkaline 1.4% agarose gel for 4 hours. The gel was washed in denaturing and neutralizing solutions before overnight transfer to Bio-rad Zeta Probe blotting paper. After crosslinking the DNA to the blotting paper with the UV stratalinker, the blot was probed with ^{32}P-DNA generated by Klenow polymerase random hexanucleotide amplification with ^{32}P-dATP with viral DNA templates. The radioactivity was detected in a GE Typhoon scanner and the bands quantified using imageQUANT software. Band intensity was compared to known standards loaded in the Southern blot to calculate the number of full length viral genomes per volume of sample.

Viral analysis

The infectivity of the viruses and chimeras were assessed via flow cytometry. $2x10^5$ B16F10 cells were seeded into 6-well plates in Gibco DMEM media with 5% fetal bovine serum (FBS) and glutamine, penicillin, and streptomycin. One day after seeding, the cells were infected with the virus diluted into 1ml of the same media with only 1% FBS. After four hours, 1ml of DMEM with 9% FBS was added to return the media to the normal 5% FBS ratio. Twenty-four hours after the initiation of infection, the cells were harvested with trypsin, fixed in 1% paraformaldehyde, permeabilized with 0.5% Triton, blocked in 10% normal goat serum in PBS, stained with mouse α-NS1 mAb (CE10B10, ref (27)) in the blocking solution, and incubated with Biolegend goat α-mouse IgG DyLight 488 secondary. Flow cytometry was performed on a MACSQuant Analyzer 10, set to record 10,000 events. The positive gate was set so that 0.5% of the uninfected, stained control cells were positive.

Transgene production

I performed the creation of the GFP-B7.1 transgene by following the Cold Spring Harbor Protocol by Szymczak-Workman et al (28). Primers were designed to amplify either GFP with the picornavirus 2A tail or 2A preceding B7.1. Two-step PCR generated the final GFP-2A-B7.1 product and it was cloned into the Topo pCR 2.1 plasmid.

Vector construction

I performed the modifications to the previous vector system to include the new GFP-B7.1 transgene and incorporate the MPV P5 NS1/NS2 sequence. Cloning was performed with restriction enzymes, quick ligase, and SURE-2 supercompetent cells.

Vector production

I performed the production of the GFP-B7.1 vector, which was created by a triple transfection of 2μg vector genome, 4μg packaging plasmid expressing VP1/VP2, and 6μg helper plasmid with adenovirus genes. After 72 hours, the cells were harvested and the vector was purified and quantitated as previously described.

Vector analysis

I analyzed the GFP-B7.1 vector with Western blots, fluorescence microscopy, and flow cytometry.

The Western blot was performed with A9 cells transfected with the GFP-B7.1 vector DNA by Superfect. Cells were harvested in lysis buffer containing protease and phosphatase inhibitors after 48 hours. The samples were boiled and the protein levels were calculated with a BCA assay. Equal amounts of protein were run on an SDS-PAGE gel and transferred to a Hybond ECL membrane, then probed with rabbit α-GFP primary pAb and α-rabbit HRP secondary. The image was generated by exposing the blot to film.

Fluorescence microscopy was performed with both vector DNA transduction by Superfect in A9 cells for 48 hours and vector particle transduction in B16F10 cells with 20,000 genomes/cell for 24 hours. Slides were fixed with 2.5% paraformaldehyde in PBS +/+, neutralized with ammonia chloride, blocked in 10% normal goat serum in PBS +/+, stained with R&D systems goat α-mouse B7.1 pAb, Invitrogen donkey α-goat IgG Alexa Fluor 594, and DAPI. Images were taken on a Zeiss Axio Imager M2 fluorescence microscope using the 20x and 40x objectives. Control slides of cells infected with virus rather than vector were treated similarly, but were permeabilized with 0.1% Triton, and stained with mouse α-NS1 mAb and goat α-mouse IgG DyLight 594.

Flow cytometry analysis of the vector was performed using the previously described flow cytometry protocol, however the samples were not permeabilized and no antibody was needed, as GFP signal was measured.

Results:

Analysis of Evolving MPV1a DNA Sequences

This project required the selection of MPV1a mutants, analysis of the genetic changes that occurred during expansion on B16F10 murine melanoma cells, isolation of the mutations that improved melanoma tropism, and their application to the vector system. Figure 4 shows the number of cells positive for viral infection at 24 hours with different parvoviruses at varying multiplicities of infection. A cell was considered positive for infection based on antibody staining for the viral protein NS1 analyzed by flow cytometry. Four viruses were used: MVMp, LuIII, MPV1a, and MPV P5. MVMp, LuIII, and MPV1a were standard stocks of virus used in the laboratory, while MPV P5 was generated by the polyclonal passage of MPV1a in B16F10 cells. At the highest multiplicity of infection with 5000 viral genomes per seeded cell, MVMp and LuIII infected <2% of the cells at 24 hours. MPV1a was more infectious with 16% of cells staining positive for NS1, while MPV P5 infected 74% of cells and led to moderate amounts of cell death and debris noticeable by microscopy. The nearly five-fold increase in 24 hour infection rates between MPV1a and MPV P5 prompted the investigation of genetic changes responsible for the increased tropism.

Before progressing to sequencing, MPV1a and MPV P5 were tested in the YUMM cell lines. While MPV P5 was selected in the classic murine melanoma B16F10 cell line, the YUMM cell lines will be used for *in vivo* experiments to allow for immunologic study, and express the most common drivers of melanomagenesis in the human disease. The genotype of YUMM1 cells is $Braf^{V600E/wt}$, $Cdkn2A^{-/-}Pten^{-/-}$, whereas that of YUMM2 cells is $Braf^{V600E/wt}$,$Pten^{-/-}$, ß-$catenin^{sta/wt}$. Figure 5 shows the results of

24 infection in the YUMM cell lines as compared to B16F10. There was a 2-fold reduction in initiation of infection at 24 hours between MPV P5 in B16F10 as compared to the YUMM cell lines. While not as infectious in YUMM cells compared to B16F10, it is clear that MPV P5 infects each of the YUMM cell lines, suggesting that passage in B16F10 cells selected for melanoma-specific "generalists", rather than for mutations specific for adapting to a host cell with the genotype of B16F10. It is also difficult to directly compare the percentage of positive cells due to the fact that different cell lines divide at different rates and S phase is required for the cell to become infected in those 24 hours. However, since it appeared that MPV P5 could infect each of the YUMM cells, we proceeded with our investigation of the genetic changes found in this virus.

Genetic analysis was performed by PCR amplification of viral DNA, ligation into cloning plasmids, and sequencing. Figure 6 shows the predicted protein sequence differences in NS1 between the published MPV1a sequence on GenBank (U12469), the parental strain of MPV1a used for selection in B16F10 cells, and the MPV P5 virus isolated after passaging. NS1, NS2, and VP1 sequence was analyzed within an approximate 2.6 kb amplified region. Clones are named from the originating virus stock, sample number, cloning plasmid used, and the date. The NS1 region was notable for one amino acid change found in all MPV P5 clones – L575S. The two mutations I206M and S529N were found in a majority of MPV P5 NS1 clones. All NS1 mutations were found before the start of NS2. Surprisingly, the mutations found in MPV P5 are identical to the GenBank sequence but differ from the parental strain of MPV1a used in the selection process. The NS2 protein sequence, including all of its spliced forms such as $NS2^{P}$, $NS2^{Y}$, and $NS2^{L}$, and VP1 were identical between all samples. Thirteen silent mutations

occurred within the fragment, but were not found in any known regions of importance, such as the NS1/NS2 splice site, localization sequences, P4 promoter, or P38 promoter. Mutations found only in one sample of the MPV1a parental or MPV P5 sequencing results were considered as PCR errors, sequencing errors, or random un-selected viral mutations and were not included in the analysis. With three amino acid mutations found in NS1, the remaining VP2 gene was sequenced as well.

Figure 7 shows the VP2 protein sequence mutations between the published MPV1a sequence on GenBank (U12469), the parental strain of MPV1a used for selection in B16F10 cells, and the resulting MPV P5 virus after passaging. As seen with the NS1 results in Figure 7, the MPV1a parental stain does not match the GenBank sequence. Only one of the twelve sequenced MPV1a parental clones matched GenBank in the VP2 region. Among the MPV P5 clones, clone "TR" denotes a nonfunctional MPV P5 VP2 clone isolated prior to my project that was never successfully used as an MVMp vector packaging capsid. Clone "TR" matches the GenBank sequence and one of the twelve MPV1a clones. Of the twelve clones that I isolated and sequenced, one clone matched the MPV1a parental strain. The remaining eleven clones exhibited varying combinations of eight mutations in the VP2 region. Three amino acid mutations occurred early in VP2 before the poly-glycine flexible region. Notable are the last two mutations -- S348N or R349K -- because most of the MPV P5 clones appear to have one of these mutations, but never both. They are also unique because of all of the amino acid mutations found in the NS1 and VP2 genes, these two were the only mutations not found in the MPV1a GenBank sequence.

The summary of mutations found between MPV1a and MPV P5 are listed in Figure 8. The localization of amino acid mutations in either NS1 or VP2 forms the basis of the following experiments, in which chimeric viruses are created with different components from NS1/NS2/VP1 and VP2. The 3' untranslated region was identical in all MPV1a parental and MPV P5 clones, and only differed from the GenBank sequence by three nucleotides. The only parts of the virus that was not evaluated was the terminal hairpins, which tend to be conserved and are difficult to clone and sequence. With the conclusion of this section, there are enough data and viral sequences to begin reconstructing the MPV1a and MPV P5 strains from clonal sequences.

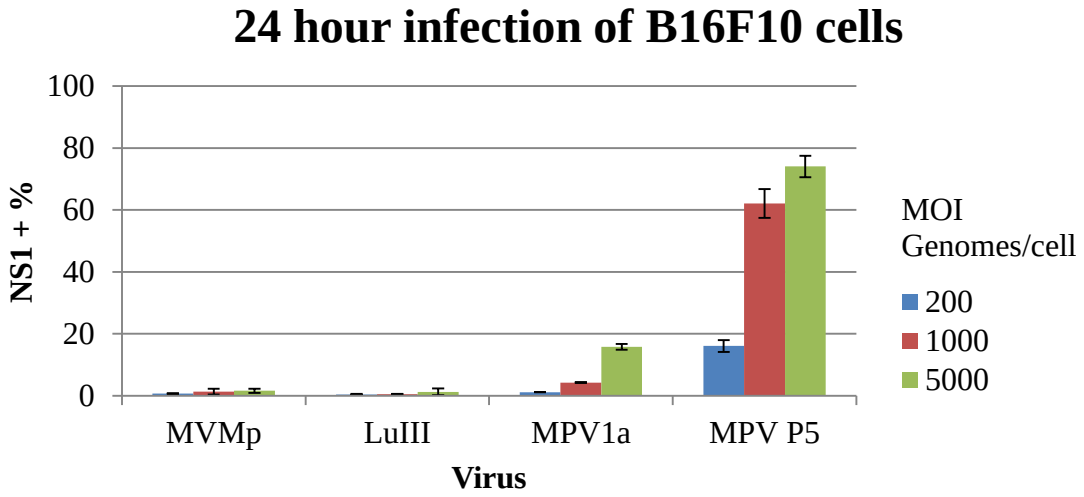

Figure 4 – Infection of B16F10 Cells with Panel of Parvoviruses

B16F10 cells were infected with varying titers of parvovirus for 24 hours. Cells were fixed, permeabilized, stained for NS1, and analyzed by flow cytometry. Stained, uninfected cells were used as the negative control to set the threshold for positive cells. Each sample was performed in duplicate. Error bars represent the standard deviation.

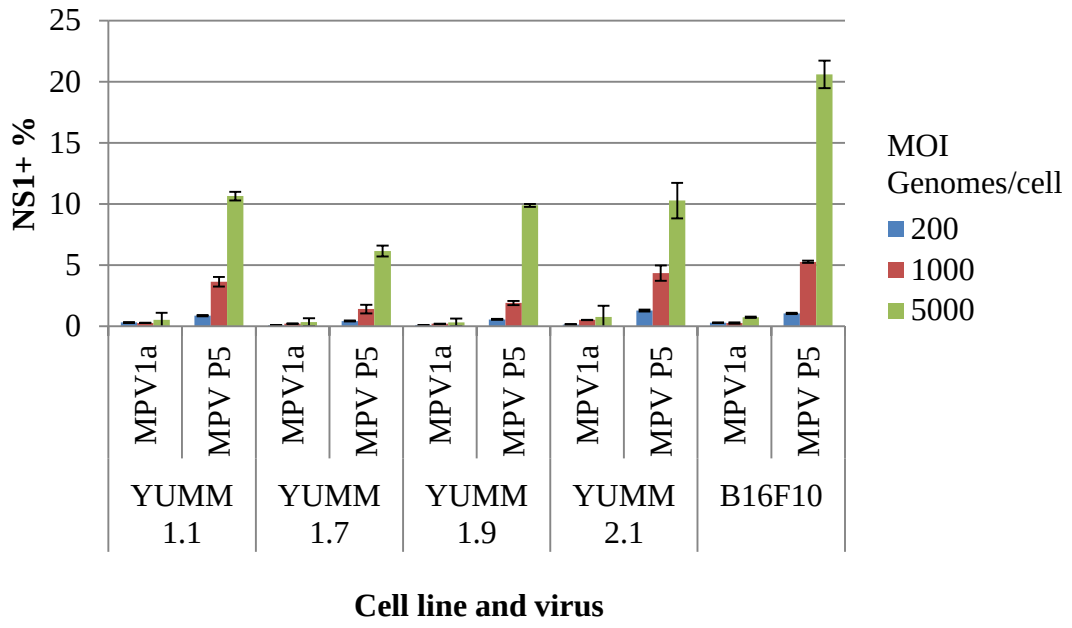

Figure 5 – Infection of YUMM cell lines with MPV1a and MPV P5

YUMM cell lines were infected with MPV1a and MPV P5 for 24 hours. Cells were fixed, permeabilized, stained for NS1, and analyzed by flow cytometry. Stained, uninfected cells were used as the negative control to set the threshold for positive cells. B16F10 cells were used as a positive control for comparison. Each sample was performed in duplicate. Error bars represent the standard deviation.

Sample	Protein Sequence NS1 Reading Frame Codons 206	529	575
MPV1a Published GenBank Seq.	M	N	S
MPV1a #01 Topo (10-20-2011)	I	S	L
MPV1a #02 Topo (10-20-2011)	I	S	L
MPV1a #03 Topo (10-20-2011)	I	S	L
MPV P5 #01 Topo (10-20-2011)	I	N	S
MPV P5 #04 NEB (09-19-2014)	M	N	S
MPV P5 #07 NEB (09-19-2014)	M	S	S
MPV P5 #08 NEB (09-19-2014)	M	N	S
MPV P5 #09 NEB (09-19-2014)	M	N	S
MPV P5 #10 NEB (09-19-2014)	I	N	S
MPV P5 #12 NEB (09-19-2014)	I	N	S

MPV1a consensus MPV P5 mutation

Figure 6 – Analysis of Coding Mutations found in NS1

Three clones from MPV1a and seven clones from MPV P5 were sequenced and compared to the published MPV1a sequence in GenBank (U12469). Coding mutations found in more than a single clone were included in the table. NS2 and VP1 protein sequence was identical between MPV1a and MPV P5. Red shading indicates the consensus sequence from the parental strain of MPV1a. Green shading indicates a mutation from the MPV1a consensus, which may or may not be the MPV P5 overall consensus.

Sample	Protein Sequence VP2 Reading Frame Codons							
	8	11	12	54	57	70	348	349
MPV1a Published GenBank	P	G	S	R	S	M	S	R
MPV1a #01 (10-01-2014)	S	R	N	K	G	I	S	R
MPV1a #02 (10-01-2014)	S	R	N	K	G	I	S	R
MPV1a #03 (10-01-2014)	S	R	N	K	G	I	S	R
MPV1a #04 (10-01-2014)	S	R	N	K	G	I	S	R
MPV1a #05 (10-01-2014)	S	R	N	K	G	I	S	R
MPV1a #06 (10-01-2014)	S	R	N	K	G	I	S	R
MPV1a #07 (10-01-2014)	S	R	N	K	G	I	S	R
MPV1a #08 (10-01-2014)	S	R	N	K	G	I	S	R
MPV1a #09 (10-01-2014)	P	G	S	R	S	M	S	R
MPV1a #10 (10-01-2014)	S	R	N	K	G	I	S	R
MPV1a #11 (10-01-2014)	S	R	N	K	G	I	S	R
MPV1a #12 (10-01-2014)	S	R	N	K	G	I	S	R
MPV P5 clone "TR" (6)	P	G	S	R	S	M	S	R
MPV P5 #01 (09-19-2014)	P	G	S	R	S	M	N	R
MPV P5 #02 (09-19-2014)	S	G	N	K	G	I	N	R
MPV P5 #03 (09-19-2014)	S	R	N	R	S	M	N	R
MPV P5 #04 (09-19-2014)	S	R	N	K	G	I	S	K
MPV P5 #05 (09-19-2014)	P	G	S	K	G	I	S	K
MPV P5 #06 (09-19-2014)	S	R	N	K	G	I	S	R
MPV P5 #07 (09-19-2014)	P	G	S	R	S	M	S	K
MPV P5 #08 (09-19-2014)	S	G	N	R	S	M	N	R
MPV P5 #09 (09-19-2014)	S	R	N	R	S	M	S	K
MPV P5 #10 (09-19-2014)	S	G	N	K	G	M	N	R
MPV P5 #11 (09-19-2014)	S	R	N	K	G	I	S	K
MPV P5 #12 (09-19-2014)	S	R	N	R	S	M	S	R

MPV1a consensus MPV P5 mutation

Figure 7 – Analysis of Coding Mutations found in VP2

Twelve clones from MPV1a and twelve clones from MPV P5 were sequenced and compared to the published MPV1a sequence in GenBank (U12469). Coding mutations found in more than a single clone were included in the table. "TR" clone is included as a nonfunctional VP2 gene used previously. Red shading indicates the consensus sequence from our parental strain of MPV1a. Green shading indicates a mutation from the MPV1a consensus, which may or may not be the MPV P5 overall consensus.

	Hairpins	**NS1**	NS2	VP1	**VP2**	3' UTR
Amino acid mutations	n/a	**3**	0	0	**8**	n/a
Silent DNA mutations	unknown	12	0	4	5	0

Figure 8 – Summary of Mutations between MPV1a and MPV P5

Coding mutations are located only in the NS1 and VP2 genes. Silent mutations were also present, although not in any known splice sites, promoter regions, or localization sequences. The 3' untranslated region (UTR) was constant between MPV1a and MPV P5. Changes in the terminal hairpins remain unknown.

Analysis of MVMp : MPV1a : MPV P5 Chimeras

Using the sequencing data, chimeric parvoviruses were assembled to assess the differences between the NS1 and VP2 mutations. The infectious clones created from MPV1a and MPV P5 served as controls, as they should perform similarly to the polyclonal stocks of MPV1a and MPV P5 analyzed by sequencing. By creating chimeras between MPV1a and MPV P5, the important mutations for B16F10 tropism were isolated. Figure 9 illustrates the construction process. During the sequencing of the MPV1a and MPV P5 viruses, restriction sites were added to the fragments to allow for reconstruction. An engineered backbone of the MVMp virus is used as the starting point due to its many built-in cloning sites and assays. The 3' UTR and hairpins are MVMp in all of the chimeras, with the NS1/NS2/VP1 and VP2 regions being replaced with MPV1a or MPV P5 sequence. The naming convention used for the remainder of this thesis is as follows: the first letter of the chimeric virus name denotes the NS1/NS2/VP1 origin, with "M" and "P" indicating MPV1a and MPV P5 respectively. The hyphen serves as the junction between NS1/NS2/VP1 and VP2. The second letter in the name denotes the origin of VP2 in the same manner of "M" or "P." Since the NS1/NS2/VP1 sequencing provided an overwhelming consensus, either MPV1a #1 or MPV P5 #8 was used in all constructs. In the VP2 region, MPV1a #1 was used as the consensus for MPV1a. MPV P5 had a variety of sequences in the VP2 region, so three clones were chosen. To maximize the number of mutations screened, and to include S348N or R349K, MPV P5 #1 and #7 were chosen. MPV P5 #11 was also chosen to see if S348N was sufficient on its own to improve infectivity. Part A shows the insertion of MPV1a or MPV P5 NS1/NS2/VP1 sequence into an MVMp backbone. This produced the two chimeras M –

MVMp and P – MVMp. Part B depicts the insertion of VP2 from either MPV1a or MPV P5 into the intermediates from Part A. The table gives the name and specific amino acid changes for each chimera. Prior to producing large quantities of the chimeric viruses, a screening experiment was performed with P – P_1 and P – P_7, where their DNAs were transfected into B16F10 cells with Superfect. After two rounds of splitting the cells as they became confluent, the culture's viability crashed, encouraging us to produce all of the chimeras since P – P_1 and P – P_7 seem to cause lytic infection.

Each chimera was produced by transfection into 293T cells with PEI. The transfections to produce chimeras with all sequence from either MPV1a or MPV P5 produced the most virus. The chimeras with alternating MPV1a and MPV P5 components produced a moderate amount of virus. The chimeras with MVMp VP2 sequence produced very little virus. After calculating the titer of each chimera by Southern blot, they were tested on B16F10 cells. Figure 10 shows the results from testing the chimeras. The percentage of B16F10 cells positive for viral infection at 24 hours after infection with polyclonal mixtures of MPV1a or MPV P5 are compared to the panel of chimeras. The experiment was performed in the same manner as Figure 4. Notable is the poor infectivity with MPV1a virus, possibly because this was an older virus stock. As for the chimeras, the chimeras with the VP2 region from MPV P5 performed the best, regardless of the NS1/NS2/VP1 region. At a multiplicity of 5000 genomes per seeded cell, M – P_1 infected 5.9% of cells and P – P_1 infected 6.3%. MPV P5 infected 27% of cells. The chimeric intermediates with VP2 from the MVMp backbone performed the worst, which correlates with them being the most difficult virus to produce.

Given the complicated nature of testing all of the chimeras, a smaller panel was selected in order to optimize timing, processing, and analysis. Figure 11 repeats the experiment performed in Figure 10 but focuses on the VP2 region from MPV P5 #1 with S348N. Neither clonal chimera performed as well as the polyclonal virus stock from which it was derived. At the highest titers of 5000 genomes per cell, M – M_1 infected 5.4% of cells at 24 hours, while MPV1a infected 15.8%. At the same titer, P – P_1 infected 44.7% of cells while MPV P5 infected 74.1%. The important component of the P – P_1 chimera appears to be the VP2 region, which increases the infectivity of M – M_1 from 5.4% to 34.1% in M – P_1. The NS1/NS2/VP1 plays a minor role in the infectivity of MPV P5, advancing M –P_1 from 34.1% to 44.7% in P – P_1. There still remains a 2-3 fold difference between the polyclonal stocks of MPV1a and MPV P5 and their cloned versions in the MVMp backbone. It is possible that we either picked the inefficient clones to use, needed to incorporate more sequence from the 3' UTR/hairpins, or that the production of the chimeras in 293T cells differed from the way that MPV1a and MPV P5 were produced in 324K and B16F10 cells, respectively.

Figure 12 shows the results from testing the P – P_1 chimera made in different cells lines. One of our major concerns was that the infectivity might vary between P – P_1 and MPV P5 due to differential processing by the cells that produced them. To test this hypothesis, the P – P_1 chimera was produced in different cell lines and compared to MPV P5. The first sample is the P – P_1 chimera, made by transfection in 293T cells, which was used in all previous experiments. It is clonally derived from plasmid DNA and undergoes a single cycle of growth in 293T cells over 72 hours and accumulates intracellularly. It is not exported into the media and may not, therefore, have been

subjected to an important late maturation step. The next sample is the same chimera made in B16F10 cells by transfection with PEI. The transfection had a low yield, but virus was collected at 72 hours. The third sample is the P – P_1 chimera from 293T cells but expanded in B16F10 cells. The virus was collected after the cells crashed and is no longer inherently clonal since selection and multiple rounds of infection occurred. The last sample is the polyclonal stock of MPV P5 that has been used throughout all of the figures and was grown in B16F10 cells. At the titer of 5000 genomes per cell, P – P_1 from 293T cells approaches 56.2% of the infectivity of MPV P5, which is consistent with the 2-fold difference seen in the previous figure. After passaging in B16F10 cells, P – P_1 is 81.3% infectious as MPV P5. The results from P – P_1 made in B16F10 cells through transfection were difficult to interpret since the titer may be inaccurate given the small amount of dilute virus produced. Overall, passaging the chimera in B16F10 cells increased the infectivity partially, but did not obtain the rate shown by MPV P5. Given that production of virus by transfection in 293T cells was not overly detrimental to its functionality, we decided to use the sequences from P – P_1 to improve the melanoma tropism of the vector system.

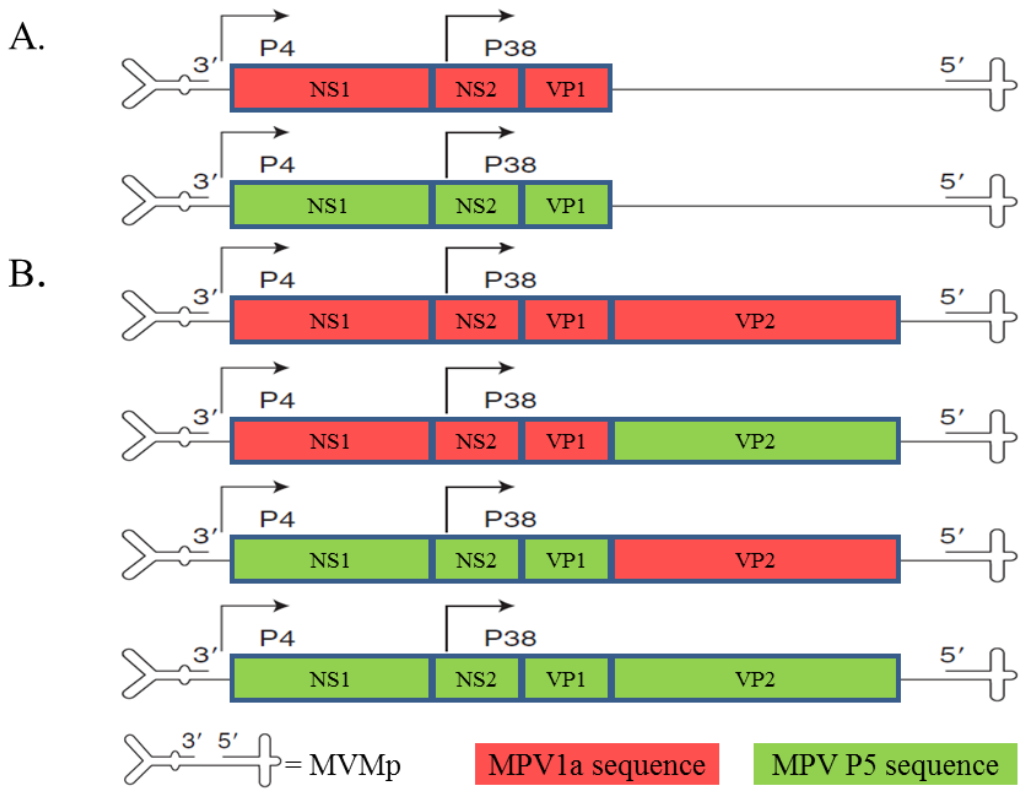

	NS1 Codon			VP2 Codon							
Name	**206**	**529**	**575**	**8**	**11**	**12**	**54**	**57**	**70**	**348**	**349**
M-M$_1$	I	S	L	S	R	N	K	G	I	S	R
M-P$_1$	I	S	L	P	G	S	R	S	M	N	R
M-P$_7$	I	S	L	P	G	S	R	S	M	S	K
M-P$_{11}$	I	S	L	S	R	N	K	G	I	S	K
P-M$_1$	M	N	S	S	R	N	K	G	I	S	R
P-P$_1$	M	N	S	P	G	S	R	S	M	N	R
P-P$_7$	M	N	S	P	G	S	R	S	M	S	K
P-P$_{11}$	M	N	S	S	R	N	K	G	I	S	K

Figure 9 – Construction of Chimeric MPV1a and MPV P5 Viruses

Chimeric viruses were created from the NS1/NS2/VP1 and VP2 fragments isolated from MPV1a and MPV P5. Part A shows how the NS1/NS2/VP1 genes were first inserted into an MVMp genome backbone. Part B shows how VP2 genes were added to Part A, resulting in eight different chimeras from one MPV1a VP2 and three MPV P5 VP2 variants. The table lists the name of each chimera and shows the differences between each construct. Naming is based on the origin of each fragment – M for MPV1a and P for MPV P5. The first letter denotes the NS1/NS2/VP1 fragment, while the second letter denotes the VP2 fragment.

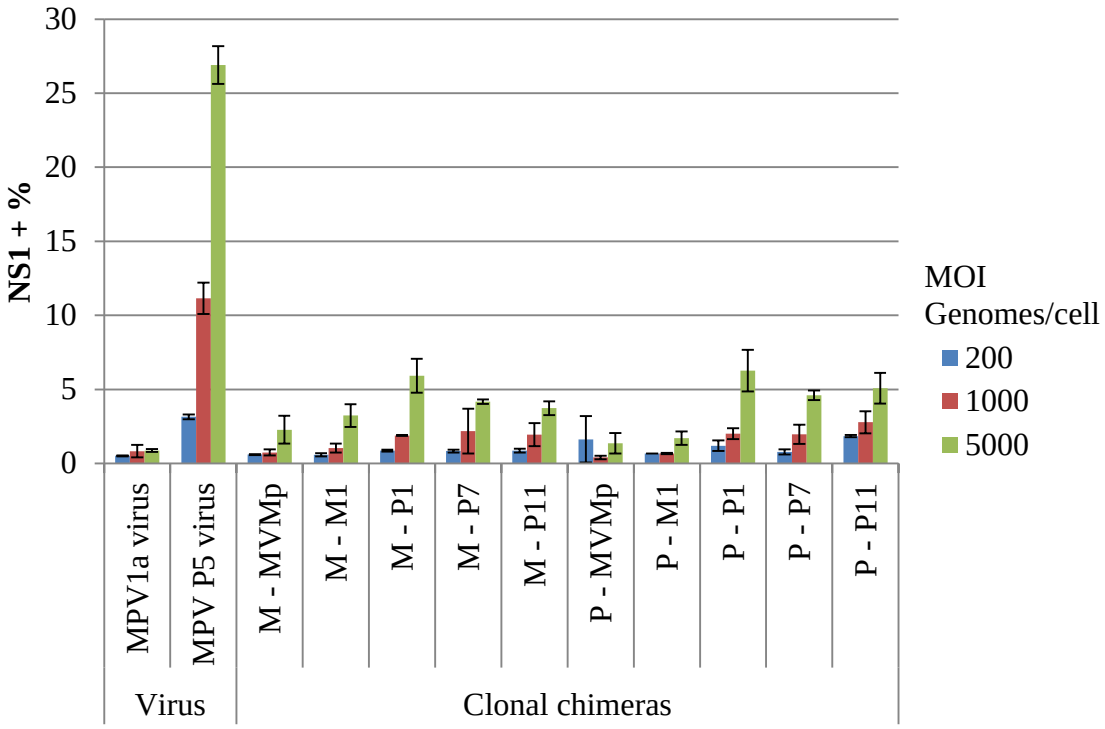

Figure 10 – Infection of B16F10 Cells with Chimeric MPV1a and MPV P5

B16F10 cells were infected with varying titers of virus for 24 hours. Polyclonal stocks of MPV1a and MPV P5 were compared to clonal chimeras. Cells were fixed, permeabilized, stained for NS1, and analyzed by flow cytometry. Stained, uninfected cells were used as the negative control to set the threshold for positive cells. Each sample was performed in duplicate. Error bars represent the standard deviation.

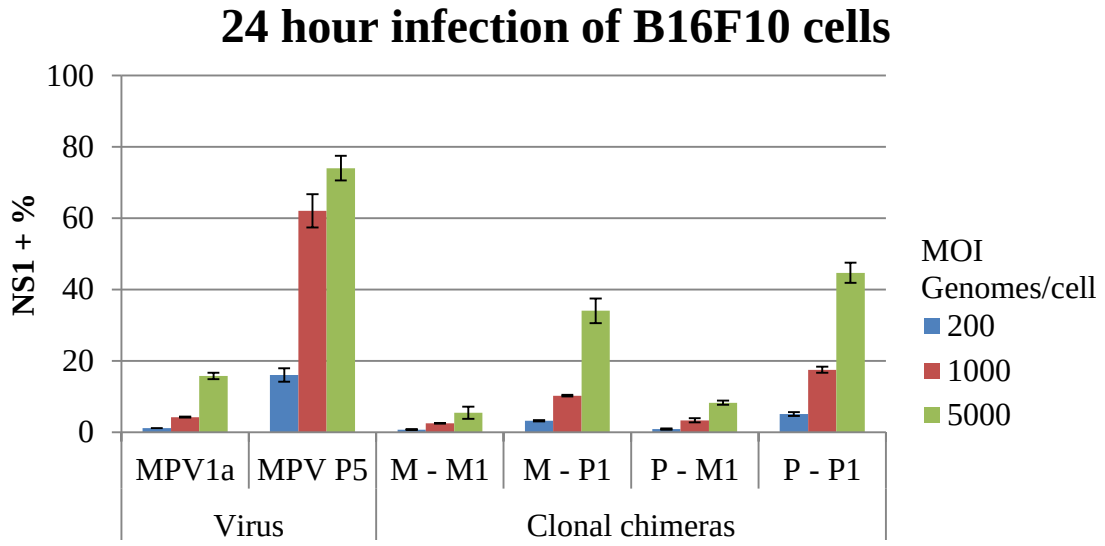

Figure 11 – Infection of B16F10 Cells with P – P_1 Chimera Components

B16F10 cells were infected with varying titers of virus for 24 hours to repeat the previous figure with fewer variables and complexity. Polyclonal stocks of MPV1a and MPV P5 were compared to components found in P – P_1. P – P_1 was used due to its relatively high infectivity relative to the other chimeras in the previous figure. Cells were fixed, permeabilized, stained for NS1, and analyzed by flow cytometry. Stained, uninfected cells were used as the negative control to set the threshold for positive cells. Each sample was performed in duplicate. Error bars represent the standard deviation.

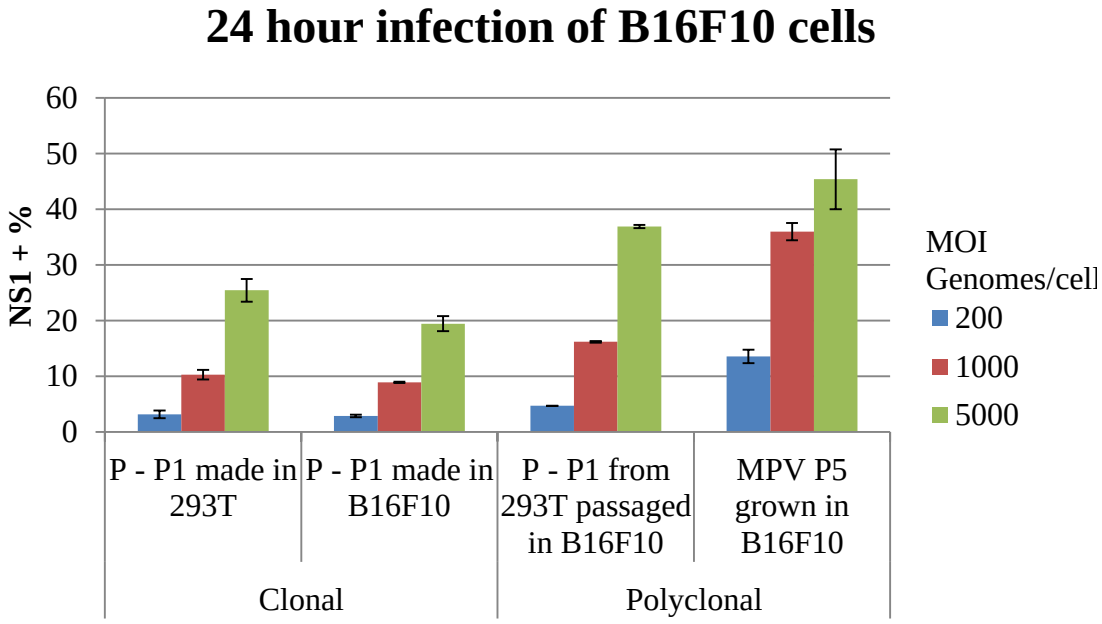

Figure 12 – Infection of B16F10 Cells with P – P_1 Produced in Different Cell Lines

The chimera P – P_1 was originally produced by a single round of replication in 293T cells. To test if 293T cells resulted in differential final processing of the mature virion, the chimera was also produced in B16F10 cells by transfection. A third sample was produced by taking the chimera from 293T cells and expanding it in B16F10 cells for multiple rounds of infection before harvesting. These three different modes of producing P – P_1 were compared to the MPV P5 stock that was grown in B16F10 cells. The infection assay was performed as previous figures.

Further Vector Development

The previous parvoviral vector system used predominantly MVMp sequence and expressed only GFP. To upgrade this vector, we decided to first express both GFP and B7.1 to make it immunostimulatory and then add MPV P5 components to improve its tropism for melanoma cells. Figure 13 shows the construction of the new vector system. Part A shows how the picornavirus sequence 2A was used to combine expression of GFP and B7.1. The sequence 2A stalls translation of mRNA into protein. The stalling process prevents peptide bond formation, and the first protein product linked to the 2A sequence is ejected from the ribosome. Translation continues, producing the second peptide independently from the first. As a result, two polypeptides can be expressed from one mRNA molecule without requiring multiple promoters or a bulky internal ribosome entry site (IRES). To incorporate the 2A sequence, two-step PCR was used to create the GFP sequence without a stop codon, linker picornavirus 2A sequence, and B7.1. Once the GAB (**G**FP – 2**A** – **B**7.1) construct was created, it was combined with a GFP-only vector system to create the intermediate in Part B. The vector system uses an early stop codon in VP1 to block its production, leading to expression of the transgene alone, once NS1 is produced and activates the P38 promoter. The intermediate construct was very large due to the increased length of B7.1 and the remaining LuIII VP2 stuffer DNA that was used to bring the original GFP-only construct up to full viral genome length (see previous Figure 3). Part C has the removal of the LuIII virus stuffer sequence that is replaced by the MVMp 3' untranslated region with two internal repeats, as normally found in MVMp. The length of GAB is approximately the same as VP2, so no additional non-specific viral "stuffer" DNA was needed to meet the 5 kb length requirement for efficient packaging of

the vector and stable capsid arrangement. Part D shows the final product, which has the NS1/NS2 region found in the chimera P – P_1. A mutant version of the B7.1 vector, named GAmB, that is incapable of costimulatory signaling due to the Y201A mutation described by Guo and colleagues (29) was also created and produced in the same manner.

Once the DNA for the vector system was produced, a preliminary test of its function was performed by plasmid transfection before undertaking the process to produce vector particles. Figure 14 shows a western blot probed for GFP. A9 cells were transfected using Superfect with either no DNA, vector DNA encoding GAB, or vector DNA encoding GFP-only. Cells were collected, lysed, and run on an SDS-PAGE gel and transferred to a Hybond ECL membrane, then probed with rabbit α-GFP primary pAb and α-rabbit HRP as secondary. The mock transfection showed no bands (Lane 1). Lane 2 shows GFP expression by the GAB vector construct. Lane 3 shows GFP expressed by a GFP-only vector, as a positive control. GFP expressed by the GAB vector should be 21 amino acids larger than normal GFP due to the tail created by the 2A linker sequence, while the GFP-only vector does not have any additional peptide attached to it. As a result, the GFP band in GAB runs slightly larger than the normal 27 kDa GFP shown in the GFP-only lane. No GFP band was seen at 82 kDa, which would be expected if the 27 kDa GFP and 55 kDA B7.1 were linked together. A western blot probed for B7.1 proved unsuccessful after several attempts, possible because the antibody works well on intact, non-permeabilized cells, but is incapable of staining denatured, lysed samples. Therefore, intact fixed cells were examined for B7.1 expression by immunofluorescence.

Figure 15 shows A9 cells transfected with GAB vector DNA using Superfect to evaluate B7.1 expression. DAPI, rabbit α-B7.1 pAb primary, and red 594nm α-rabbit

secondary were applied to fixed, non-permeabilized cells. The cells were examined by fluorescence microscopy, where blue represents DAPI staining of nuclear DNA, green for GFP, and red for B7.1. The fourth image shows the merged result of all three previous images. The DAPI image shows multiple nuclei of A9 cells on the spot slide. The GFP image highlights a single cell that has the majority of its intensity at the center of the cell. The B7.1 image shows staining on the outside of the cell clearly marking its dentritic-like extensions. Finally, the merged image emphasizes the blue nucleus, GFP on the inside of the cell, and B7.1 exposed on the surface.

Given the success of the western blot in Figure 14 confirming slightly larger-than-normal GFP and Figure 15 showing B7.1 expression on the cell surface, we proceeded to form vector particles by packaging the vector DNA in the MPV P5 capsid.

Figure 16 shows the construction of the vector particle. Three plasmids were used in a triple transfection to generate dual transgene vector particles in 293T cells. The first plasmid, named P – P_1 GAB 2R vector, has an MVMp backbone (hairpins and 3'UTR with two repeats) with the MPV P5 NS1/NS2 from the P – P_1 chimera, a truncated VP1 sequence from LuIII, and the GFP-B7.1 transgene. This plasmid, when expressed, creates NS1/NS2 from the P4 promoter. NS1 drives the P38 promoter in the vector creating the GFP and B7.1 proteins. NS1 also drives the P38 promoter in the P – P_1 packaging plasmid. This plasmid has the C-terminal sequence of LuIII NS1/NS2 that includes the P38 promoter, followed by the VP1/VP2 genes from the P – P_1 chimera. The poly-adenylation signal from rabbit ß-globin replaces the viral 3'UTR in order to eliminate any homology between this region in both the vector and the packaging plasmid. As a result, capsid proteins expressed from the packaging plasmid can assemble

and encapsidate the vector DNA that is incapable of making capsid. The third plasmid encodes the viral genes VA, E2A, and E4 from adenovirus that have been shown to improve AAV vector formation (30) and also improves parvoviral vector trans-encapsidation as well. The diminished sequence identity between the plasmids suppresses recombination and reduces the risk of generating propagation-competent virus.

Once the vector particles were produced, they were first tested on B16F10 cells seeded on microscope slides. Previous immunofluorescence images used A9 cells, whereas here we are testing B16F10 cells with vector particles packaged in the P – P_1 capsid. B16F10 cells were incubated with 20,000 vector particles per cell for 24 hours. Figure 17 shows microscopy images of B16F10 cells that were uninfected, infected with P – P_1, or infected with GAB. In Part A, the cells were permeabilized and stained for NS1 in red. The uninfected control shows no expression of GFP or NS1. P – P_1 shows expression of NS1 but no GFP. The GAB vector shows expression of both GFP and NS1. This confirmed that cells infected with the vector could be identified with GFP as an alternative to permeabilizing and staining for NS1. Another set of spot slides as shown in Part B were prepared in parallel and were fixed but not permeabilized. They were stained with goat α-B7.1 pAb and red α-goat secondary. Uninfected cells and P – P_1 infected B16F10 cells show neither GFP nor B7.1, while GAB-infected cells express both. Since the GAB vector functioned well, we decided to quantitate the transduction rate of the vector particles.

Figure 18 shows the transduction rate of the P – P_1 GAB vector compared to infection rate of the P – P_1 chimera. Since the same components were utilized in both

constructs, the rates should be the same. B16F10 cells were exposed to 20,000 genomes per cell of either the vector or chimera for 24 hours. Vector-transduced cells were analyzed for GFP signal, while cells infected by the chimera were fixed and stained for NS1. Rates of expression in the cells were 33% and 23% for the vector and chimera, respectively. The chimera values showed considerable variation, such that no significant difference was seen between the two infection efficiencies.

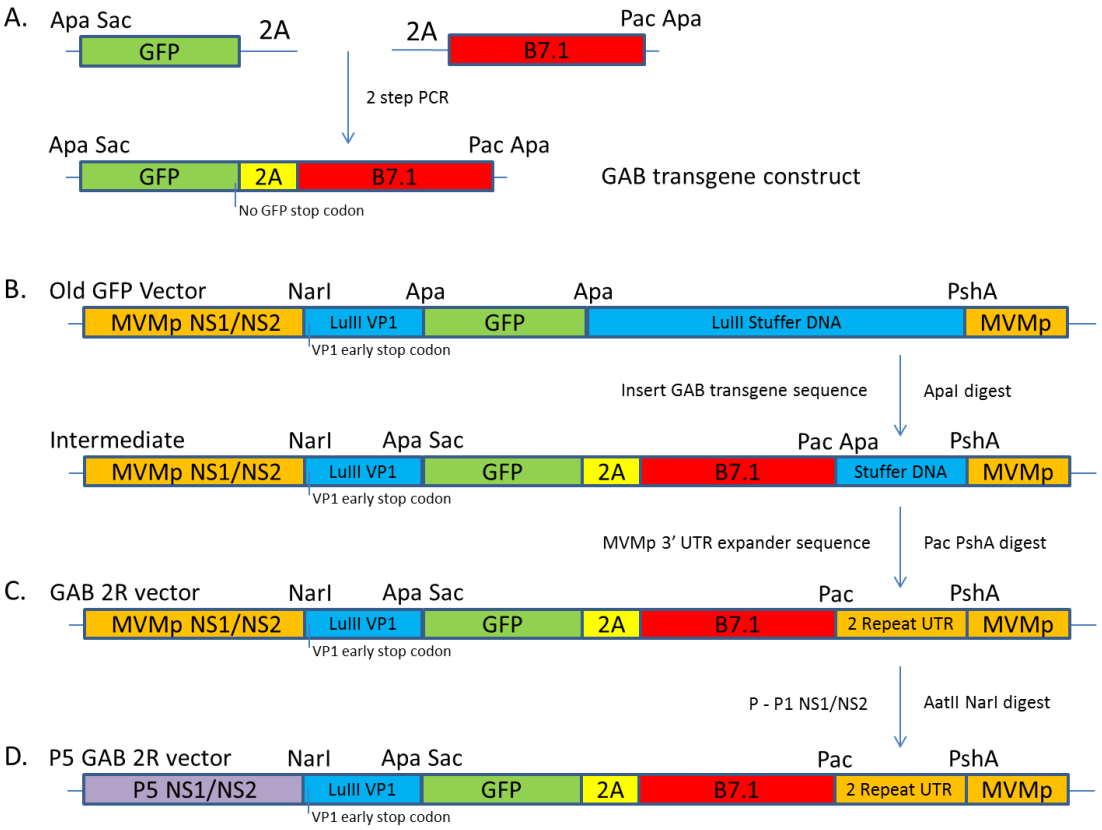

Figure 13 – Production of the GFP-B7.1 Vector Construct

An MVMp GFP-expressing vector was altered to express GFP and B7.1 with the MPV P5 NS1/NS2 region from the P – P_1 chimera. Part A shows how two-step PCR combined GFP and B7.1 into a single reading frame with a picornavirus 2A linkage. The 2A sequence stalls the ribosome during translation, leading to separate GFP and B7.1 peptides despite a single mRNA transcript. This construct of **G**FP, 2**A**, and **B**7.1 is named "GAB." Part B shows the original vector system with an early VP1 stop codon to promote transgene expression and the replacement of GFP in the vector by GAB. Part C shows the removal of LuIII stuffer DNA used to bring the GFP-only vector to full genome length. Part D shows the incorporation of the NS1/NS2 region of P – P_1 to improve the melanoma tropism of the vector.

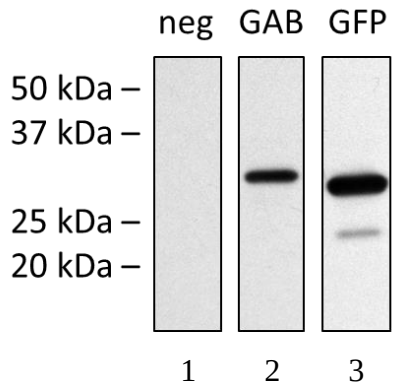

Figure 14 – Western Blot Analysis of GFP Expression by Vector DNA Transfection

A9 cells were transfected using Superfect with either no DNA, GAB, or GFP-only vector DNA. Cells were harvested 48 hours later. Staining for GFP showed no signal in the negative control (lane 1). The GFP band from GAB transfection (lane 2) was slightly larger than the GFP-only vector positive control (lane 3) due to the additional peptides from the 2A linker that are connected to the end of GFP.

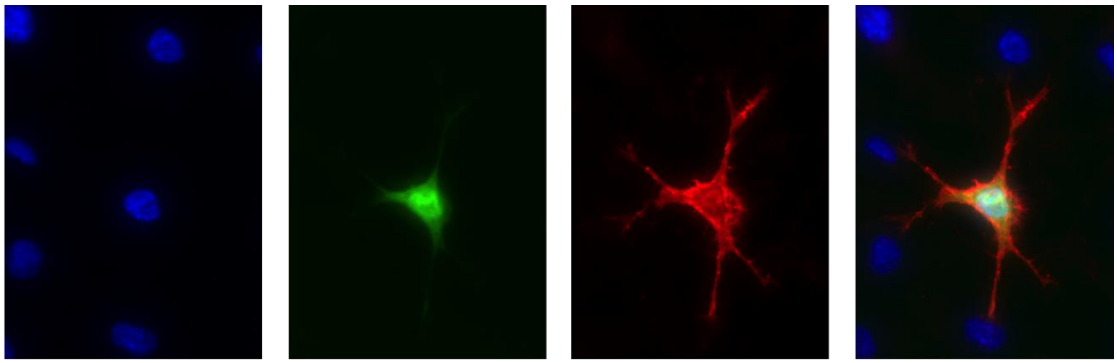

DAPI GFP B7.1 Merged

Figure 15 – Fluorescence Microscopy of GAB Vector DNA Transfection

A9 cells were transfected using Superfect with GAB vector DNA. Cells were fixed 48 hours later and stained for B7.1. The DAPI image shows blue nuclear staining. GFP expression shows green intracellular fluorescence. B7.1 expression shows antibody staining of the cellular membrane in non-permeabilized cells.

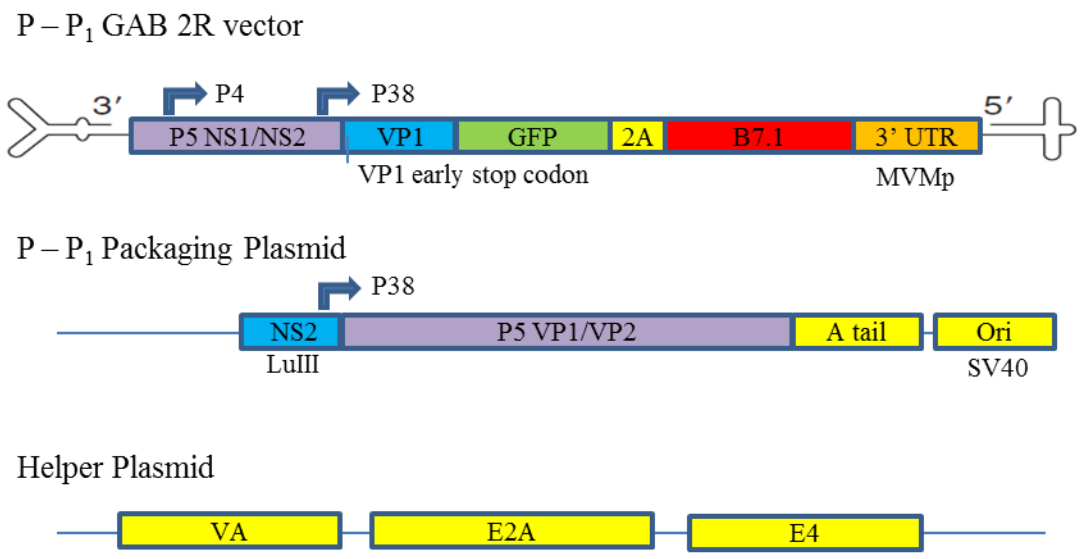

Figure 16 – GAB Vector Production

Given the success of the DNA transfection in A9 cells, the GAB vector was produced with the VP1/VP2 genes from the P – P_1 chimera. This is achieved by a triple transfection with the vector genome, packaging plasmid, and an adenovirus helper plasmid to improve efficiency. The vector genome generates NS1, which activates the P38 promoter. VP1/VP2 from the packaging plasmid is expressed to provide the capsid for the vector genome.

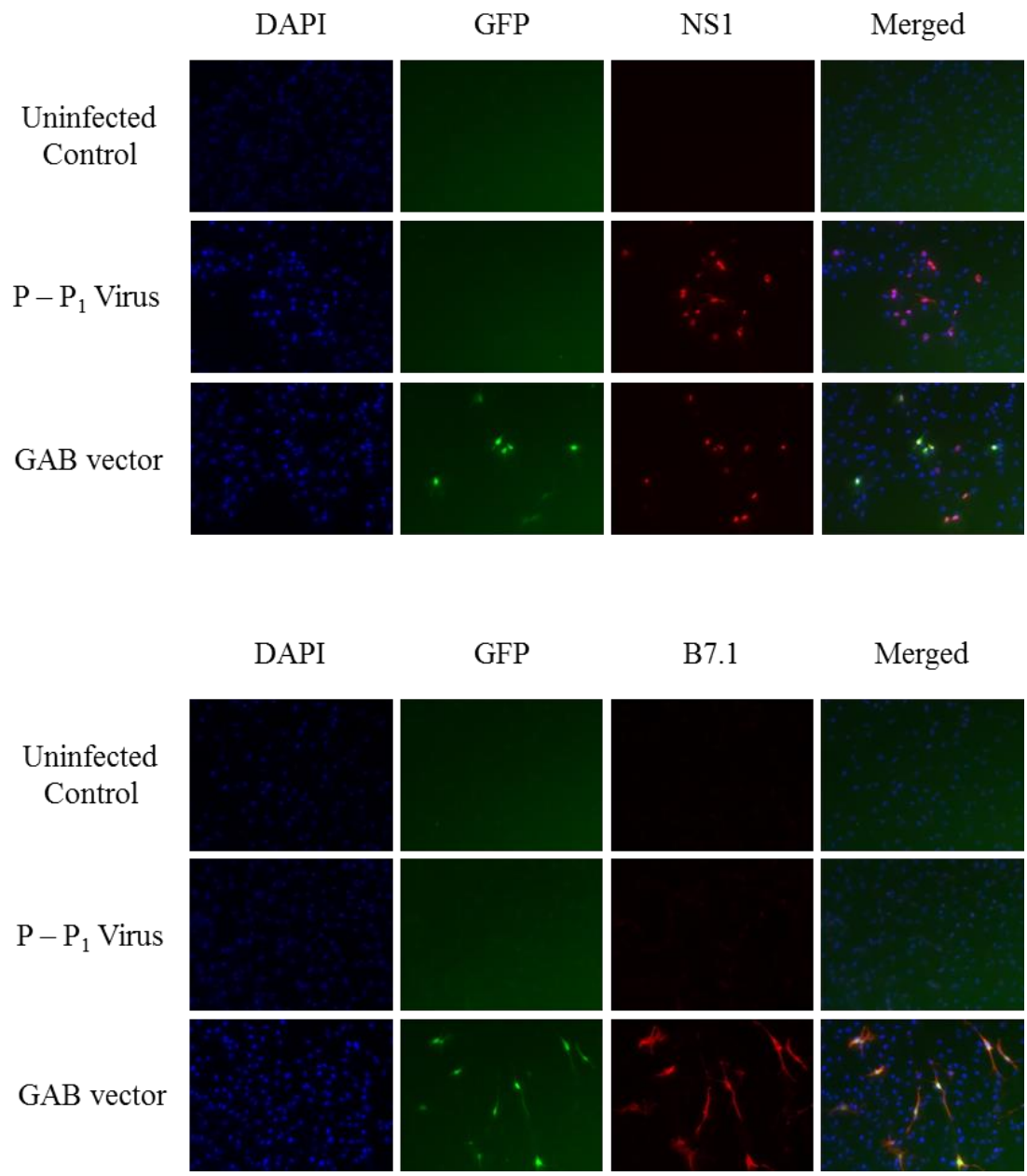

Figure 17 – Vector Transduction of B16F10 Cells

B16F10 cells seeded on spot slides were infected with 20,000 genomes per cell of P – P_1 chimera or the P – P_1 GAB vector for 24 hours and then were fixed. The first panel shows cells permeabilized and stained for NS1 in the red channel. The uninfected control shows no GFP or NS1, the P – P_1 chimera shows NS1 only, and the GAB vector produces GFP and NS1. The second panel shows staining for B7.1 in non-permeabilized cells. The uninfected control and P – P_1 chimera show no GFP or B7.1, while the GAB vector expresses both.

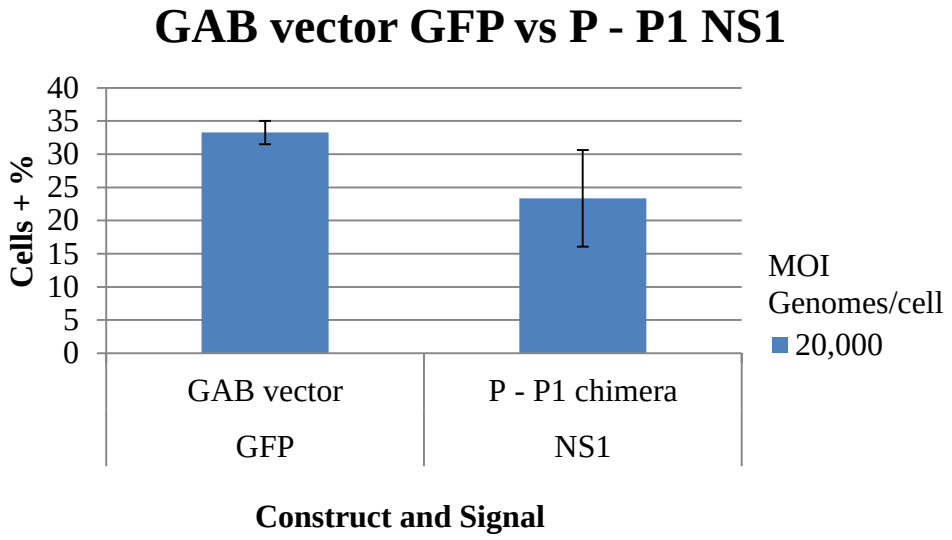

Figure 18 – Flow Cytometry Analysis of GAB Vector Compared to P – P_1 Chimera

B16F10 cells were infected with 20,000 genomes per cell of the P – P_1 GAB vector or P – P_1 chimera for 24 hours and were fixed. Cells transduced with the GAB vector were analyzed for GFP signal. Cells infected with the P – P_1 chimera were permeabilized and stained for NS1. Each sample was performed in duplicate with uninfected cells as the negative control. Error bars represent the standard deviation.

Discussion:

The overarching goal for this project was to create the most efficient vector for the transduction of immunostimulatory genes into murine melanoma cells. To do this, we investigated an MPV P5 mutant parvovirus that was selected by serial passage in the B16F10 mouse melanoma cell line. Multiple themes arose from this goal as we experimented with the MPV P5 virus and tried to make a clonal sequence that would perform like the polyclonal mixture from which it was derived.

Process of Selection

The process of selection used in generating MPV P5 was very non-specific. Simply, the viral sub-species that was able to replicate and spread most rapidly would continue to increase in the overall proportion of the viral mixture. While this would be ideal for an oncolytic vision for parvoviral treatment of melanoma, this is not the best suited approach for optimizing the vector system, since the vector replicates but does not expand in culture. Therefore, it is possible that we have selected MPV P5 to become the fastest replicating, or the fastest packaged, or the fastest exported virus. What we need is the virus that initiates infection the best, meaning that a low multiplicity of virus would cause the highest percentage of cells to become infected during a single round of infection. However, the evidence suggests that we unknowingly created a virus that incentivized rapid expansion in cell culture.

Analysis of MPV P5

The goal of analyzing MPV P5 was to extract the necessary components to make a functioning vector, and the VP2 region was initially our primary interest. However, after many failed attempts at creating a clonal version of MPV P5 that used its VP2

region in an MVMp backbone, the search was expanded to include the NS1/NS2/VP1 regions as well. In retrospect, the so-called "TR" clone that was used extensively before this project lacked one of the two VP2 mutations that have subsequently been identified as being important for MPV P5 tropism.

Early attempts at using PCR to create entire genome copies of MPV P5 were unsuccessful, and cloning the genome in separate halves proved to be more straightforward. At this point, we contemplated using deep sequencing to get thousands of sequence reads, but we decided against it for several reasons. First, after sequencing, we wanted to be able to use whichever sequence appeared to be the consensus. This was much easier done with a few PCR products that were put into plasmids and sequenced. Second, deep sequencing would not show us how the mutations occurred in individual copies of the genome. As we discovered that MPV P5 tended to either have S348N or R349K in the VP2 gene, this would have been lost in the aggregated data from deep sequencing. So the decision was made to use PCR to generate clones for sequencing.

The process of PCR presented some problems. First, the primers were designed from the published MPV1a sequence in GenBank. As a result, if the tropism-defining mutations were at the beginning of NS1, end of VP1, start of VP2, or end of VP2, the primer would mask the mutation. Second, splitting the genome in half could mean that we lost the correlation of mutations in the left half that have co-evolved with mutations in the right half.

Rational and Results from the MPV P5 Chimeras

Ideally, clonal versions of MPV1a and MPV P5 would have been generated that functioned like their polyclonal parents. However, both the $M - M_1$ and $P - P_1$ chimeras

failed to be as infectious as their parents. The idea behind generating so many chimeras was to isolate the necessary genetic features to incorporate into the vector. Originally, we thought it would be more straightforward to clone the VP2 region directly into the packaging plasmid if the VP2 region was found to be the only important component. As the chimeric virus data became more complicated, it became easier to clone all of the P – P_1 components into the vector system to fit with our goal of creating the most efficient melanomatropic vector, rather than characterizing specific mutations responsible for the tropism change.

Since the chimeras were not as infectious as MPV P5, we questioned our decision not to include the MPV P5 3' UTR or hairpins in the constructs. For many reasons, the 3' UTR was largely ignored. We knew that the UTR did not mutate from MPV1a to MPV P5, so that made it less interesting. Also, the UTR had 2 internal repeats and is similar to the MVMp sequence in construct backbone. The addition of difficult cloning sites in the MPV P5 3' UTR was also a major deterrent. However, now that we have the P – P_1 chimera that still underperforms compared to its uncloned parent, we have to consider that it is, perhaps, more important that we originally thought. This is reinforced by the fact that both M – M_1 and P – P_1 were unable to replicate at the rate of their polyclonal ancestors. Since no changes were found between MPV P5 and its parent in the 3' UTR, this region is likely important for the overall functionality of MPV1a, rather than increasing its infectivity specifically in melanoma cells. The smaller internal repeats found in the 3' UTR of MPV1a/MPV P5 may perform better with the chimera and vector genomes than the MVMp 3' UTR. Historically, the 3' UTR was thought of as just a stuffer sequence to make the genome the right size to appropriately fill the viral capsid,

since a full capsid is necessary to give the mature virion its durability. Evolutionarily, the internal repeats appear to be capable of expanding or shrinking in response to size changes in the rest of the genome. However, there is now evidence of the 3' UTR mutating and changing in length when the virus is grown in different cell lines, even though the genome is packaged into the same capsid, indicating that the 3' UTR contributes more significantly to viral tropism than previously thought.

The other component that was largely ignored in this process were the terminal hairpins. They are notoriously difficult to work with due to the hairpin structures creating problems with sequencing and cloning. Their small size and complementarity means that they can be easily and undetectably deleted and are extremely difficult to amplify by PCR. Also, the fact that they are strongly conserved within genera suggested that they are an unlikely source of variation, either between MVM and MPV1a, or between MPV1a and its MPV P5 derivatives. However, just as with the 3' UTR, the observation that we were unable to make M – M_1 perform like MPV1a despite having a very strong consensus sequence indicated that some part of the genome derived from the MVMp backbone in the chimera is suboptimal for the overall functionality of the MPV1a clone.

A surprising detail from the sequencing was how our parental strain of MPV1a failed to match the published sequence. It was even more surprising that subsequent selection on B16F10 cells shifted MPV P5 closer to the published sequence. This may have occurred because MPV1a is a murine virus originally isolated and grown in the L3 murine clonal T cell line and had been packaged in human 324K cells to amplify stocks over time (31). It is possible that unintentional selection on 324K cells led to the

differences seen between the published sequence and polyclonal MPV1a we sequenced. When selection began on murine B16F10 cells, MPV P5 may have drifted back to the original published sequence, except for the addition of S348N and R349K, which were not seen in the published sequence or the sequence we derived for the parental MPV1a. The lack of S348N or R349K mutations in the VP2 of the published sequence or parental MPV1a suggests that these changes are the most significant adaptations to efficient growth in murine melanoma cells.

The effects of VP2 surface residues has been studied in MVMp. In MVMp, 60 VP subunits assemble into a T=1 icosahedral particle. The capsid polypeptides assemble as a repeating triangular unit bordered by 5-fold, 3-fold, and 2-fold axes. The 5-fold axis is located at the pore where viral DNA is packaged into and extruded from the capsid. The 3-fold axis has been identified as the location of a neutralizing antibody epitope. The depression at the 2-fold axis is responsible for glycan binding and has been shown to be important for tropism in MVM. MVMp and MPV1a share 71.2% homology of VP2 protein sequence (9) and we may be able to use the MVMp structure to help decode the MPV1a mutations. An MVMp surface map of VP2 residues (see Figure 19A) is helpful to see which residues are exposed on the surface of the virion and could influence tropism (32). By locating the mutations found in MPV P5, we can see if the mutated residues interact with known tropism-determining residues within the MVMp structure. To get oriented, Figure 19B shows four MVMp VP2 subunits arranged to re-construct the 2-fold symmetry axis in PyMOL with PDB structure 1Z14. Figure 19C enlarges the 2-fold axis region, as outlined by the blue boxes in Figures 19A and 19B. Of the eight VP2 mutations found in MPV P5, S348N and R349K (shown in white text as MVMp

residues) would be on the surface of the virion and near the tropism-defining residues (shown in black text). A limitation of this method of analysis is that there may be significant conformational differences between the known structure of MVMp and the unknown structure of MPV P5. Although the overall structure of VP2 is predicted to be similar, individual residues may not align. Not surprisingly, the known tropism-defining residues in MVMp are different in MPV P5 as well. For example, residue K241, which appears very close to R349, is a serine in MPV P5. Therefore, the tropism-defining residues shown in the figure are not the actual residues of MPV P5. The creation of more chimeras with single amino acid changes could further explain the question of tropism, however the main objective was to use MPV P5 sequence to make a vector, so dissection of the mutations was not followed to exhaustion.

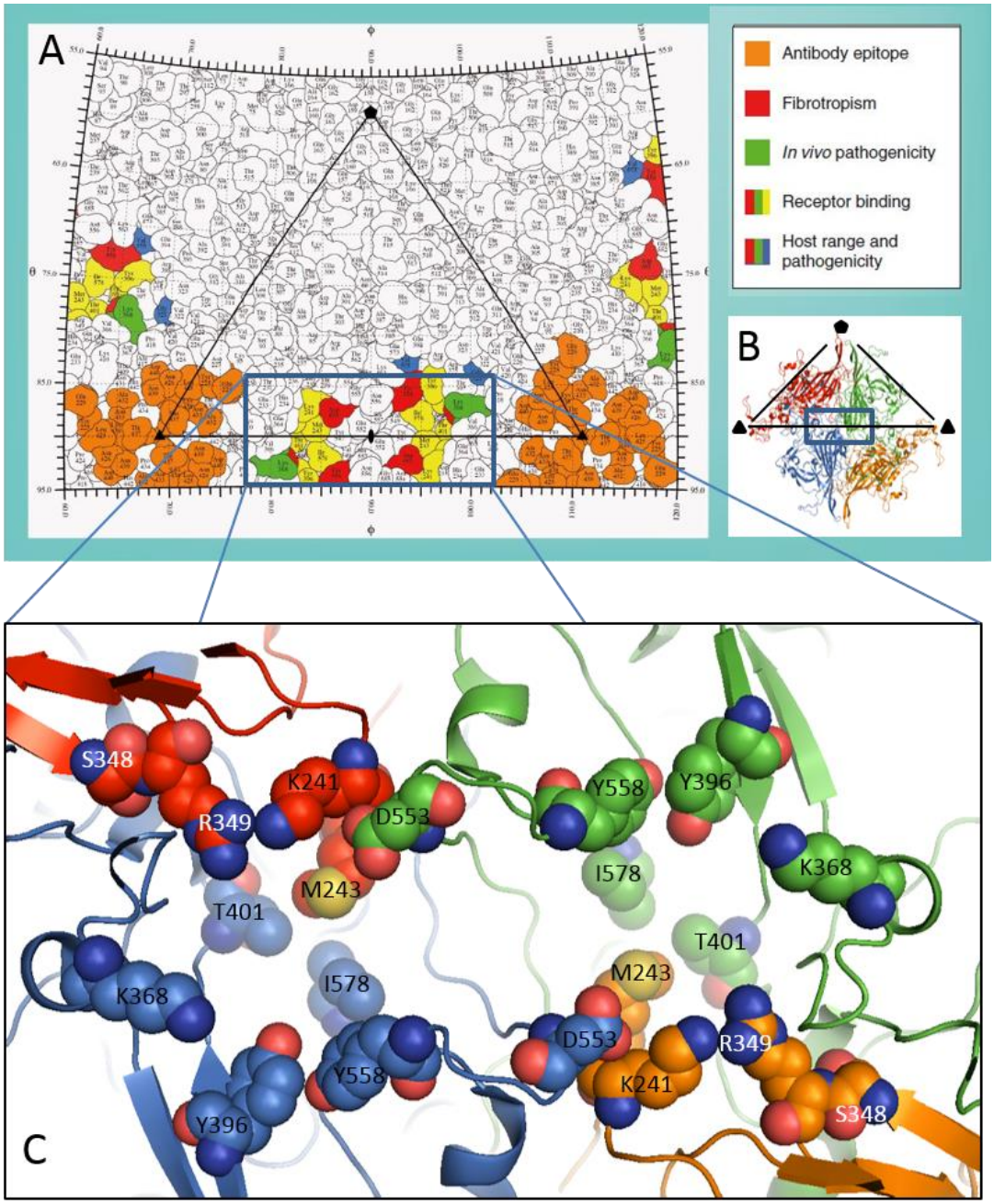

Figure 19 – VP2 Mutation Analysis

The role of VP2 in determining tropism has been extensively studied using MVMp. Part A is a figure from Halder & Agbandje-McKenna (31) which shows the surface residues of the VP2 protein exposed on the outside of the virion. The residues responsible for tropism and receptor binding are clustered along the 2-fold axis of the triangular unit. Part B shows how four VP2 peptides align along the 2-fold axis in MVMp. The colors of the subunits are preserved in Part C, which highlights the proximity of mutated residue positions in MPV P5 (white text) with the known residues important for tropism in MVMp, as determined by Part A (black text).

Creating the Vector

Until now, the parvoviral vectors created in our lab have expressed only one protein. The use of the picornavirus 2A sequence provided a unique opportunity to fit two genes in a compact space without requiring an additional, bulky internal ribosome entry site. The 2A sequence has been studied extensively and equipped with addition sequence to optimize the stalling and peptide breakage process. This system has also been shown to generate a reliable 1:1 ratio of first and second products (33). We decided that GFP should be the first transgene due to the reported problem of "slip-streaming" with the 2A sequence whereby the intracellular localization of the second product follows that of the first product. By putting GFP first, it can be expressed into the cytosol, and the B7.1 protein can still be targeted to the cell membrane. GFP serves as a useful reporter due to the extensive permeabilization required to stain for viral proteins in the nucleus. Once we can confirm B7.1 signal with GFP in transduced cells by flow cytometry, GFP can be used as a surrogate for NS1 or B7.1, allowing us to ask more complex questions.

So far, the picornavirus 2A sequence has worked flawlessly. Western blots confirmed the slightly larger GFP molecule due to the 2A tail on it, and the immunofluorescence of transduced cells showed intracellular GFP coinciding with membrane-bound B7.1 under the microscope. The vector genome packaged well into the $P - P_1$ capsid proteins at a reasonable yield. The one major problem that remains is optimizing the signal for analysis by flow cytometry. In contrast to the immunofluorescence results, the GFP positive cells do not appear to be staining significantly positive for B7.1 by flow analysis. However, I believe this remains a

protocol problem that will require optimization of the cell processing, antibodies, and staining parameters.

Adapting the P – P_1 chimera into the vector system was straightforward, and we expected similar rates of transduction with the vector as infection with the chimera, since all of the chimera components were used in the vector. MPV P5 NS1/NS2 was used in the vector genome, while MPV P5 VP1/VP2 was expressed from the packaging plasmid. The 3' UTR and hairpins have been consistently MVMp sequence in both the chimeras and vector, but could be upgraded to MPV P5 sequence should they be found to be important in ongoing 3' UTR experiments.

Such improvements in vector transduction efficiency, if achieved, would allow us to move to more immunologic assays. We plan to use the vector in a murine melanoma YUMM cell derivative that expresses the melanocyte protein GP100, a known tumor antigen in human melanomas, and is transplantable into mice. This will allow us to use MHC I tetramer technology to measure the induction of cytotoxic T cells by vector transduction *in vivo*. We also intend to examine whether the virus and/or the vector lead to cellular changes that signal the immune system through DAMPs and PAMPs.

Conclusion

MPV1a virus that was grown in B16F10 cells mutated over time and became significantly more infectious for these cells. By cloning and sequencing parts of the genome, we were able to construct a chimeric parvovirus infectious clone that was able to infect B16F10, albeit not as efficiently as the selected virus from which it was derived. The VP2 gene was the most important region for conferring B16F10 tropism. Using the components of the chimeric virus, a vector was developed to co-express GFP and the co-

stimulatory molecule B7.1. With more testing and improvement, this vector could be used to induce melanoma cells to express this immunostimulatory molecule, and thus augment the use of antibody treatments currently used to block inhibitory signals.

References:

1. Siegel RL, Miller KD, and Jemal A. Cancer statistics, 2015. *CA: a cancer journal for clinicians.* 2015;65(1):5-29.

2. Rotte A, Bhandaru M, Zhou Y, and McElwee KJ. Immunotherapy of melanoma: Present options and future promises. *Cancer metastasis reviews.* 2015.

3. Leung J, and Suh WK. The CD28-B7 Family in Anti-Tumor Immunity: Emerging Concepts in Cancer Immunotherapy. *Immune network.* 2014;14(6):265-76.

4. Martin-Fontecha A, Cavallo F, Bellone M, Heltai S, Iezzi G, Tornaghi P, Nabavi N, Forni G, Dellabona P, and Casorati G. Heterogeneous effects of B7-1 and B7-2 in the induction of both protective and therapeutic anti-tumor immunity against different mouse tumors. *European journal of immunology.* 1996;26(8):1851-9.

5. Sule-Suso J, Arienti F, Melani C, Colombo MP, and Parmiani G. A B7-1-transfected human melanoma line stimulates proliferation and cytotoxicity of autologous and allogeneic lymphocytes. *European journal of immunology.* 1995;25(10):2737-42.

6. Townsend SE, Su FW, Atherton JM, and Allison JP. Specificity and longevity of antitumor immune responses induced by B7-transfected tumors. *Cancer research.* 1994;54(24):6477-83.

7. Coughlin CM, Wysocka M, Kurzawa HL, Lee WM, Trinchieri G, and Eck SL. B7-1 and interleukin 12 synergistically induce effective antitumor immunity. *Cancer research.* 1995;55(21):4980-7.

8. Haile ST, Bosch JJ, Agu NI, Zeender AM, Somasundaram P, Srivastava MK, Britting S, Wolf JB, Ksander BR, and Ostrand-Rosenberg S. Tumor cell programmed death ligand 1-mediated T cell suppression is overcome by coexpression of CD80. *Journal of immunology.* 2011;186(12):6822-9.

9. Cotmore SF, and Tattersall P. In: Karl Maramorosch AJS, and Frederick AM eds. *Advances in virus research.* Academic Press; 2007:183-232.

10. Cotmore SF, and Tattersall P. Parvoviruses: Small Does Not Mean Simple. *Annual Review of Virology.* 2014;1(1):517-37.

11. Cotmore SF, and Tattersall P. Parvovirus diversity and DNA damage responses. *Cold Spring Harbor perspectives in biology.* 2013;5(2).

12. Grekova S, Zawatzky R, Horlein R, Cziepluch C, Mincberg M, Davis C, Rommelaere J, and Daeffler L. Activation of an antiviral response in normal but

not transformed mouse cells: a new determinant of minute virus of mice oncotropism. *Journal of virology.* 2010;84(1):516-31.

13. Paglino JC, Andres W, and van den Pol AN. Autonomous parvoviruses neither stimulate nor are inhibited by the type I interferon response in human normal or cancer cells. *Journal of virology.* 2014;88(9):4932-42.

14. Mattei LM, Cotmore SF, Tattersall P, and Iwasaki A. Parvovirus evades interferon-dependent viral control in primary mouse embryonic fibroblasts. *Virology.* 2013;442(1):20-7.

15. Wildner O. Oncolytic viruses as therapeutic agents. *Annals of medicine.* 2001;33(5):291-304.

16. Hersey P, and Gallagher S. Intralesional immunotherapy for melanoma. *Journal of surgical oncology.* 2014;109(4):320-6.

17. Maxwell IH, Terrell KL, and Maxwell F. Autonomous parvovirus vectors. *Methods.* 2002;28(2):168-81.

18. Dupont F. Risk assessment of the use of autonomous parvovirus-based vectors. *Current gene therapy.* 2003;3(6):567-82.

19. Rommelaere J, Geletneky K, Angelova AL, Daeffler L, Dinsart C, Kiprianova I, Schlehofer JR, and Raykov Z. Oncolytic parvoviruses as cancer therapeutics. *Cytokine & growth factor reviews.* 2010;21(2-3):185-95.

20. Ball-Goodrich LJ, Moir RD, and Tattersall P. Parvoviral target cell specificity: acquisition of fibrotropism by a mutant of the lymphotropic strain of minute virus of mice involves multiple amino acid substitutions within the capsid. *Virology.* 1991;184(1):175-86.

21. Spalholz BA, and Tattersall P. Interaction of minute virus of mice with differentiated cells: strain-dependent target cell specificity is mediated by intracellular factors. *Journal of virology.* 1983;46(3):937-43.

22. Paglino J, Burnett E, and Tattersall P. Exploring the contribution of distal P4 promoter elements to the oncoselectivity of Minute Virus of Mice. *Virology.* 2007;361(1):174-84.

23. Vollmers EM, and Tattersall P. Distinct host cell fates for human malignant melanoma targeted by oncolytic rodent parvoviruses. *Virology.* 2013;446(1-2):37-48.

24. Cotmore SF, Agbandje-McKenna M, Chiorini JA, Mukha DV, Pintel DJ, Qiu J, Soderlund-Venermo M, Tattersall P, Tijssen P, Gatherer D, et al. The family Parvoviridae. *Archives of virology.* 2014;159(5):1239-47.

25. Mattei LM, Cotmore SF, Li L, Tattersall P, and Iwasaki A. Toll-like receptor 9 in plasmacytoid dendritic cells fails to detect parvoviruses. *Journal of virology.* 2013;87(6):3605-8.

26. Damsky WE, Curley DP, Santhanakrishnan M, Rosenbaum LE, Platt JT, Gould Rothberg BE, Taketo MM, Dankort D, Rimm DL, McMahon M, et al. beta-catenin signaling controls metastasis in Braf-activated Pten-deficient melanomas. *Cancer cell.* 2011;20(6):741-54.

27. Yeung DE, Brown GW, Tam P, Russnak RH, Wilson G, Clark-Lewis I, and Astell CR. Monoclonal antibodies to the major nonstructural nuclear protein of minute virus of mice. *Virology.* 1991;181(1):35-45.

28. Szymczak-Workman AL, Vignali KM, and Vignali DA. Design and construction of 2A peptide-linked multicistronic vectors. *Cold Spring Harbor protocols.* 2012;2012(2):199-204.

29. Guo Y, Wu Y, Zhao M, Kong XP, and Liu Y. Mutational analysis and an alternatively spliced product of B7 defines its CD28/CTLA4-binding site on immunoglobulin C-like domain. *The Journal of experimental medicine.* 1995;181(4):1345-55.

30. Matsushita T, Elliger S, Elliger C, Podsakoff G, Villarreal L, Kurtzman GJ, Iwaki Y, and Colosi P. Adeno-associated virus vectors can be efficiently produced without helper virus. *Gene therapy.* 1998;5(7):938-45.

31. Ball-Goodrich LJ, and Johnson E. Molecular characterization of a newly recognized mouse parvovirus. *Journal of virology.* 1994;68(10):6476-86.

32. Halder S, Ng R, and Agbandje-McKenna M. Parvoviruses: structure and infection. *Future Virology.* 2012;7(3):253-78.

33. Kim JH, Lee SR, Li LH, Park HJ, Park JH, Lee KY, Kim MK, Shin BA, and Choi SY. High cleavage efficiency of a 2A peptide derived from porcine teschovirus-1 in human cell lines, zebrafish and mice. *PloS one.* 2011;6(4):e18556.